Preface

Riemann surfaces appear in many branches of mathematics and physics, as in differential and algebraic geometry and the theory of moduli spaces, in topological field theories, quantum chaos and integrable systems. The practical use of Riemann surface theory has been limited for a long time by the absence of efficient computational approaches. In recent years considerable progress has been achieved in the numerical treatment of Riemann surfaces which stimulated further research in the subject and led to new applications. The existing computational approaches follow from the various definitions of Riemann surfaces: via non-singular algebraic curves, as quotients under the action of Fuchsian or Schottky groups, or via polyhedral surfaces.

It is the purpose of the present monograph to give a coherent presentation of the existing computational approaches to Riemann surfaces. The authors of the contributions are representants from all groups developing publically available numerical codes in this field. The monograph is directed to graduate students and researchers working on applications of Riemann surfaces. Publically available software as part of the Algebraic Curves package in Maple and the Riemann Surface java package as part of jtem are explained for typical examples. Thus this monograph illustrates which software tools are available and how they can be used in practice. In addition many graphical examples for solutions to partial differential equations and in surface theory will be presented.

In the introduction, A. Bobenko presents a comprehensive summary of the theory of compact Riemann surfaces, Abelian differentials, periods on Riemann surfaces, theta functions and uniformization techniques. Riemann originally introduced Riemann surfaces as the compactification and desingularization of plane algebraic curves. B. Deconinck and M. Patterson have followed this approach together with M. v. Hoeij for a number of years. They have devised several algorithms facilitating different aspects of the effective computation with Riemann surfaces represented by plane algebraic curves. Their algorithms have led to the *algcurves* Maple package: a collection of Maple programs for computations with algebraic curves and Riemann sur-

faces. This package is included with the main Maple distribution. B. Deconinck and M. Patterson describe their algorithms, the Maple implementations and how to use them for instructive examples, as well as new features which are to be distributed with future releases of Maple. The numerical approach via algebraic curves involves the computation of contour integrals on the Riemann surface. To study the moduli spaces associated to Riemann surfaces numerically, a more efficient computation of these integrals is necessary. J. Frauendiener and C. Klein present a fully numerical approach based on numerically optimal Gauss integration which provides a very efficient method of high accuracy. Riemann surfaces also appear in the explicit solution of certain integrable partial differential equations fow which concrete examples are discussed. The code is available as a Matlab package at `http://math.u-bourgogne.fr/IMB/klein/codes.html`.

A complementary approach to compact Riemann surfaces is based on the quotients of the action of certain groups and uniformization theory. M. Schmies discusses numerics of the Schottky uniformization of Riemann surfaces and in particular the convergence of Poincaré theta series and their use in the numerical treatment of Riemann surfaces which are incorparated in the freely available Java project *jtem*. For typical examples from surface theory, the use of the *jtem* package, which is freely available at `www.jtem.de`, is described. R. Hidalgo and M. Seppälä discuss Schottky and Fuchsian uniformizations of hyperelliptic algebraic curves. Using a method originally due to Myrberg, they construct an algorithm that approximates the generators of a Schottky group uniformizing a given hyperelliptic algebraic curve. Using quasiconformal mappings, one can numerically pass from a Schottky uniformization to a Fuchsian uniformization. An important application of Riemann surfaces is the treatment of multiply connected domains. D. Crowdy and J. Marshall study conformal mappings for multiply connected domains both analytically and numerically. They discuss a new formula for the Schwarz-Christoffel mapping to multiply connected polygonal boundaries in terms of the Schottky-Klein prime function. The latter function is numerically evaluated by using Schottky uniformization.

The relation of Riemann surfaces to polyhedral surfaces offers yet another computational approach. A. Bobenko, C. Mercat and M. Schmies discuss the computation of period matrices of Euclidean surfaces by methods of discrete differential geometry. The latter are based on the notions of discrete holomorphicity and discrete Riemann surfaces. An interesting object associated to the modular space of Riemann surfaces are determinants of Laplacians. These determinants appear in topological field theories and quantum chaos. A. Kokotov presents a review on determinants of Laplacians on Riemann surfaces in polyhedral metrics.

Berlin, Dijon,   *Alexander Bobenko*

august, 2008

Christian Klein

Contents

Part I

Introduction

Part II

Algebraic Curves

Computing with plane algebraic curves and Riemann surfaces: the algorithms of the Maple package "algcurves"

Bernard Deconinck[1] and Matthew S. Patterson[2]

[1] Department of Applied Mathematics, University of Washington
     Seattle WA 98195-2420, USA
     `bernard@amath.washington.edu`
[2] William G. Pritchard Fluid Mechanics Laboratory,
     Department of Mathematics,
     Penn State University,
     University Park, PA 16802, USA
     `mpatters@amath.washington.edu`

1 Introduction

In this chapter, we present an overview of different algorithms for computing with compact connected Riemann surfaces, obtained from desingularized and compactified plane algebraic curves. As mentioned in Chapter 1, all compact connected Riemann surfaces may be represented this way. The maple package "algcurves", largely developed by the authors and Mark van Hoeij contains implementations of these algorithms. A few recent additions to the "algcurves" package are not due to the authors or Mark van Hoeij. The algorithm behind those commands are not discussed here as they have no bearing on anything associated with Riemann surfaces.

Because some of the algorithms presented here are algebraic in nature, they rely on exact arithmetic, which implies that the coefficients of the algebraic curves are required to have an exact representation. Most importantly, floating point numbers are not allowed as coefficients for these algorithms. The reason for not allowing floating point numbers is that the geometry of the Riemann surface is highly dependent on the accuracy of the coefficients in its algebraic curve representation. If an algebraic curve has singularities, then, almost surely, the nature of these singularities will be affected by inaccuracies in the coefficients of the curve. This may affect the algebraic algorithms discussed below, such as those for the calculation of the genus, homology and holomorphic 1-forms on the Riemann surface. Users of the "algcurves" package can consider floating point coefficients, but these need to be converted to a different form (rational, for instance), before the programs will accept the

input. Furthermore, since we are using algebraic curves to represent Riemann surfaces, the algebraic curves are always considered over the complex numbers. Throughout this chapter, "calculation" is used when exact results are obtained, whereas "computation" is used for numerical results.

Apart from the restriction to an exact representation, all of the algorithms discussed in detail in this chapter are general in the sense that they apply to all compact connected Riemann surfaces. An appendix is presented discussing the use of a few algorithms that apply to a restricted class of algebraic curves and Riemann surfaces, such as elliptic and hyperelliptic surfaces. This appendix contains many examples, but no detailed explanation of the specifics of the algorithms.

All of the descriptions of the algorithms of the main body of this chapter are preceded by the next section which outlines the connection between plane algebraic curves and Riemann surfaces with a level of detail appropriate for what follows. The work reviewed here may be found in [DvH01, DP07a, DP07b, vH95, vH94]. The examples of the implementations use commands available in Maple 11 (Released Spring 2007). A few identified commands are used that are not available in Maple 11 yet.

2 Relationship Between Plane Algebraic Curves and Riemann Surfaces

In this section, some required background from the theory of Riemann surfaces is introduced. More details can be found in such standard references as [FK92, Spr57]. Excellent places to read up on Riemann surfaces and how they relate to plane algebraic curves that do not require an extensive background are the monographs by Brieskorn and Knörrer [BK86] and Griffiths [Gri89].

Consider a plane algebraic curve, defined over the complex numbers $\mathbb{C}$, i.e., consider the subset of $\mathbb{C}^2$ consisting of all points (x, y) satisfying a polynomial relation in two variables x and y with complex coefficients:

$$f(x, y) = a_n(x)y^n + a_{n-1}(x)y^{n-1} + \ldots + a_1(x)y + a_0(x) = 0. \qquad (1)$$

Here $a_j(x)$, $j = 0, \ldots, n$ are polynomials in x. Write $a_j(x) = \sum_i a_{ij}x^i$, where the coefficients a_{ij} are complex numbers. Assuming $a_n(x) \not\equiv 0$, n is the degree of $f(x, y)$ considered as a polynomial in y. We only consider irreducible algebraic curves, so $f(x, y)$ cannot be written as the product of two nonconstant polynomials with complex coefficients.

Let d denote the degree of $f(x, y)$ as a polynomial in x and y, i.e. d is the largest $i + j$ for which the coefficient a_{ij} of $x^i y^j$ in $f(x, y)$ is non-zero. The behavior at infinity of the algebraic curve is examined by homogenizing $f(x, y) = 0$ by letting

$$x = X/Z, \quad y = Y/Z, \tag{2}$$

and investigating

$$F(X, Y, Z) = Z^d f(X/Z, Y/Z) = 0. \tag{3}$$

Here $F(X, Y, Z)$ is a homogeneous polynomial equation of degree d. Finite points $(x, y) \in \mathbb{C}^2$ on the algebraic curve correspond to triples $(X : Y : Z)$ with $Z \neq 0$. Since for these points $(X : Y : Z) = (X/Z : Y/Z : 1)$, we may equate $Z = 1$, so finite points can be denoted unambiguously by (x, y) instead of $(X/Z, Y/Z)$. Points at infinity correspond to triples $(X : Y : Z)$, with $Z = 0$. Hence, at a point at infinity, at least one of the two coordinate functions x or y is infinite. Because $F(X, Y, 0)$ is a homogeneous polynomial of degree d, there are at most d points at infinity.

The algebraic curve can have singular points. An algorithm to efficiently calculate the singular points of an algebraic curve is discussed in Sect. 5. Here we briefly discuss singularities as they need to be dealt with to transition from an algebraic curve to a Riemann surface. Finite singular points on the algebraic curve specified by $f(x, y) = 0$ satisfy $f(x, y) = 0 = \partial_x F(x, y) = \partial_y F(x, y)$. Points at infinity can also be singular. Singular points at infinity satisfy $\partial_X F(X, Y, Z) = \partial_Y F(X, Y, Z) = \partial_Z F(X, Y, Z) = 0$ (then also $F(X, Y, Z) = 0$, by Euler's theorem for homogeneous functions). Desingularizing the algebraic curve results in a Riemann surface, i.e., a one-dimensional complex-analytic manifold (so it is two-dimensional over the real numbers; it is a surface). There are various ways of desingularizing algebraic curves. Our methods use Puiseux series, as detailed in Sect. 3. Each nonsingular point on the algebraic curve corresponds to one place on the Riemann surface, whereas a singular point on the algebraic curve can correspond to multiple places on the Riemann surface.

In what follows, Γ is used to denote the Riemann surface obtained by desingularizing and compactifying (by adding the places at infinity) the algebraic curve represented by $f(x, y) = 0$. All Riemann surfaces obtained this way are connected (because $f(x, y)$ is irreducible) and compact (because the points at infinity are included). Conversely, as stated in Chapter 1 it is known that every compact connected Riemann surface can be obtained this way [BBE$^+$94, Spr57]. From here on out, all Riemann surfaces considered are understood to be connected and compact. We use $\hat{\Gamma}$ to denote the compactified algebraic curve, including its singularities. Further, we use the term "point" to denote a value in the complex x-plane. On the other hand, "place" is used to denote a location on the Riemann surface Γ, or, unambiguously, a location on the desingularized plane algebraic curve.

3 Puiseux Series

Many of the algorithms presented in the next sections use the ability to work efficiently with the local behavior near a given place on an algebraic curve. For

our algorithms, this local behavior is understood using Puiseux expansions. These expansions allow us to distinguish between regular points, branch points and singular points. Further, in addition to determine the nature of singular points, Puiseux expansions characterize the topology of an algebraic curve near branch points. One way to look at this is that Puiseux series are our way to desingularize the algebraic curves we are working with. There are other ways of doing so, all with their advantages and disadvantages. A popular alternative is the use of quadratic transformations to "lift" the singular plane algebraic curve to a higher-dimensional nonsingular curve [Abh90].

Newton's Theorem, which we summarize below, completely describes the local behavior of a plane algebraic curve. Over the neighborhoods of a regular point $x = \alpha$ the coordinate function y is given locally as a series in ascending powers of $x - \alpha$ [Bli66]. Near a branch point however, y is given necessarily by a series with ascending fractional powers in $x - \alpha$. Such series are known as *Puiseux series*. It is common to choose a local parameter, say t, such that x and y are written as Laurent series in that local parameter[1]. That is, if α is a branch point of order r, then $t^r = x - \alpha$, and y is written as a Laurent series in t. A pair $(x(t), y(t))$ is referred to as a Puiseux expansion as it is equivalent to a Puiseux series.

Newton's Theorem. In a lifted neighborhood of $x = \alpha$, the n y-roots of (1) are determined by a finite number of pairs of expansions of the form

$$P_j = \left(x = \alpha + t^{r_j}, y = \beta_j t^{s_j} + \beta'_j t^{s'_j} + \cdots \right). \tag{4}$$

with $r_j, s_j, s'_j, \ldots \in \mathbb{Z}$, $t \in \mathbb{C}$, $\alpha, \beta_j, \beta'_j, \ldots \in \mathbb{C}$. Here (i) $|r_j|$ is the number (the *branching number*) of y-roots that merge at place P_j. If $|r_j| > 1$ for one of the P_j, then α is a branch point and P_j is a branch place. (ii) For $|t| > 0$, a place P_j represents r_j distinct y-values and $\sum_j r_j = n$. (iii) The coefficients $\beta, \beta', \ldots$ are all non zero; only a finite number of the integer exponents $s_j < s_{j'} < \ldots$ are negative; and no common factor $|r_j|$ divides all of $s_j, s_{j'}, \ldots$. (iv) For places over $\alpha = \infty$, $\alpha = 0$ and $r < 0$. Thus $x = 1/t^{-r}$. A Puiseux expansion evaluated at $t = 0$ is called a *center*.

The algorithm to compute Puiseux expansions implemented in the "algcurves" package is essentially that described by Newton in letters to Oldenburg and Leibniz [BK86]. A treatment of the algorithm with much detail may be found, for instance, in [Wal62] where it is presented as a constructive proof of the algebraic closure of Puiseux series. At base, the calculation of Puiseux expansions is an exercise in algebraic asymptotics. The paper by van Hoeij [vH94] discusses a modern implementation of the algorithm, most importantly providing a method allowing one to determine how many terms

---

[1] For finite points, only Taylor series in the local parameter are required. Laurent series with a finite number of singular terms are necessary to encompass points at infinity.
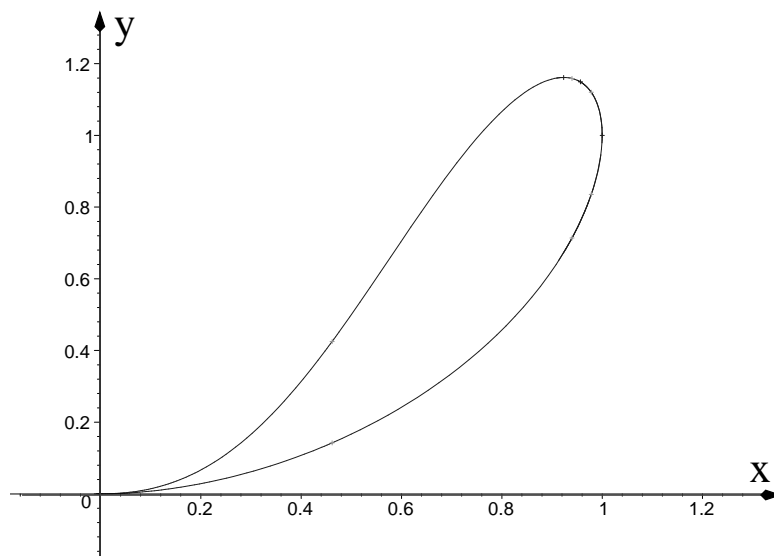
Fig. 1. The real graph of the Ramphoid cusp curve.

of the expansions are required to guarantee distinct branches are recognized as such.

Example. Consider the curve

$$f(x, y) = (x^2 - x + 1)y^2 - 2x^2y + x^4 = 0. \tag{5}$$

Note that for this example $a_n(x) = x^2 - x + 1 \neq 1$, complicating the calculation of Puiseux expansions [Bli66]. Nevertheless, such computations are still possible. The curve (5) is known as a "ramphoid cusp" because of the structure of the real part of the graph at the origin [Wal62], as shown in Figure 1. The graph was produced using the command `plot_real_curve` of the "algcurves" package. We compute the local structure of this curve at two different x-values. First we compute the expansions over $x = 0$, which is not a root of a_n, and second, the expansions over one of the roots of $a_n(x) = 0$.

The command `puiseux` used below computes the y-expansions of $f(x, y) = 0$ over $x = 0$. The fourth argument being zero implies that the procedure calculates as many terms as are necessary to distinguish separate expansions.

```
># read in the package
>with(algcurves):
```

```
># define the algebraic curve
>f:=x^4+x^2*y^2-2*x^2*y-y^2*x+y^2:
># compute the Puiseux expansions over x=0
>puiseux(f,x=0,y,0);
```

$$\left\{ x^2 + x^{5/2} \right\}$$

Note that $x = 0$ is a branch point by virtue of the fractional power in the second term. This one expansion represents two distinct places for $|x| > 0$. To recover both roots near $x = 0$ one conjugates the series using the r-th roots of unity, where r is the greatest common denominator of the exponents of the series. Thus, one makes the r substitutions $x \mapsto e^{2\pi i j/r} x$, $j = 1, \ldots, r$. In this case, the $r = 2$ different y-roots are

$$y = \left\{ x^2 + x^{5/2} + \cdots , x^2 - x^{5/2} + \cdots \right\}.$$

If, instead of 0, the fourth argument is specified to be a positive integer value M, then the expansions are computed up to x^M. For example, if $M = 4$, then the $x^{7/2}$ term is included, but terms of order x^4 and higher are not.

```
>puiseux(f,x=0,y,4);
```

$$\left\{ x^2 + x^{5/2} + x^3 + \frac{1}{2} x^{7/2} \right\}$$

```
>puiseux(f,x=0,y,5);
```

$$\left\{ x^2 + x^{5/2} + x^3 + \frac{1}{2} x^{7/2} - \frac{5}{8} x^{9/2} \right\}$$

Including a fifth argument t in the call to `puiseux` changes the output. In this case the output is a pair of expansions in the local parameter t.

```
>f:=x^4+x^2*y^2-2*x^2*y-y^2*x+y^2:
># compute the Puiseux expansions using local coordinate t
>puiseux(f,x=0,y,0,t);
```

$$\{[x = t^2, y = t^4 + t^5]\}$$

4 Integral Basis

We start by explaining the concept of an integral basis. Integral bases are used in all aspects of algebra, but they have become particularly important with the rise of computer algebra systems, as their construction often allows the convenient calculation of many other derived quantities. An example of this in our chapter is the use of the integral basis for the calculation of the holomorphic 1-forms on a Riemann surface, see Section 9. Another example is their use in the algorithmic integration in finite terms of algebraic functions.

Consider the coordinate functions x and y on the Riemann surface Γ. These two functions are algebraically dependent, by the defining equation $f(x, y) = 0$. Denote by $A(\Gamma)$ the part of the Riemann surface where both x and y are finite. Also, let $O_{A(\Gamma)}$ be the set of all meromorphic functions on the Riemann surface that have no poles in $A(\Gamma)$ (*i.e.*, $O_{A(\Gamma)}$ is the set of all quotients of polynomials in x and y such that their combination is well defined for all finite singularities). For example, $O_{A(\Gamma)}$ contains $\mathbb{C}[x, y]$, the set of all polynomials in x and y: since in $A(\Gamma)$ both x and y are finite, any polynomial of x and y results in a finite value as well. If the algebraic curve has no finite singularities, then every meromorphic function on the Riemann surface without poles in $A(\Gamma)$ can be represented as a polynomial in x and y, hence $O_{A(\Gamma)} = \mathbb{C}[x, y]$ if the curve has no finite singularities. In general, $O_{A(\Gamma)}$ is the integral closure of $\mathbb{C}[x, y]$ in the meromorphic functions on A: it is the set of all meromorphic functions g on $A(\Gamma)$ which satisfy a monic polynomial equation

$$g^m + \gamma_{m-1}(x, y)g^{m-1} + \ldots + \gamma_1(x, y)g + \gamma_0(x, y) = 0, \tag{6}$$

for a certain positive integer m and coefficients $\gamma_i(x, y)$, $i = 0, 1, \ldots, m - 1$ which are in $\mathbb{C}[x, y]$. Note that $m = 1$ implies $\mathbb{C}[x, y] \subset O_{A(\Gamma)}$, so all polynomials in x and y are in $O_{A(\Gamma)}$. An integral basis $\{\beta_0, \ldots, \beta_{n-1}\}$ of O_A can be computed such that every element of O_A can be written as a linear combination of $\beta_0, \ldots, \beta_{n-1}$ with coefficients that are polynomial in x.

An efficient method to calculate an integral basis of $O_{A(\Gamma)}$, using Puiseux expansions, is given in [vH94]. The algorithm is as follows: we put $\beta_0 = 1$. To construct β_k, $k = 1, \ldots, n - 1$, we repeat the following steps:

1. Guess $\beta_k = y^k$. Actually, the algorithm in [vH94] uses $\beta_k = y\beta_{k-1}$, which is more efficient. The examples below are easier to work out with $\beta_k = y^k$. The results, of course, are equivalent.
2. We define V to be the set of all elements v, modulo the linear combinations of β_j, $j = 1, \ldots, k$, where the coefficients of the linear combinations are polynomial in x. Here v is of the form

$$v = \sum_{j=0}^{k} w_j(x)y^j, \tag{7}$$

where the $w_j(x)$ are rational functions of x, such that v is regular on $A(\Gamma)$.

3. If V is not empty, we choose an element $\hat{v}$ of V of the form

$$\hat{v} = \frac{\sum_{j=0}^{k} \hat{w}_j(x)\beta_j}{k(x)}, \qquad (8)$$

where $\hat{w}_j(x)$, $j = 1, \ldots, k$ and $k(x)$ are polynomial in x. Also, $\hat{w}_k(x) \equiv 1$.
4. We replace our guess for β_k with $\hat{v}$, and repeat from step 2.

It is shown in [vH94] that the set V becomes smaller at every step, thus the algorithm terminates. We now briefly discuss this method using two examples.

Example. Consider the algebraic curve defined by

$$f(x, y) = y^3 - x^7 + 2x^3 y = 0. \qquad (9)$$

This curve has one finite singular point at $(x, y) = (0, 0)$. The Puiseux expansions at this point are

$$P_1 : (x = t, y = t^4/2 + \ldots), \quad P_2 : (x = -2t^2, y = 4t^3 + \ldots). \qquad (10)$$

- We start with $\beta_0 = 1$.
- Our first guess for $\beta_1 = y$. With this guess, the set V consists of all elements $v = w_0(x) + w_1(x)y$ that do not contain any polynomial part that is of first degree in y. Since we are interested in the behavior at the origin, we can represent v as

$$v = \frac{w_{0,-1}}{x} + \frac{w_{0,-2}}{x^2} + \ldots + \frac{w_{0,-p}}{x^p} + \left(\frac{w_{1,-1}}{x} + \frac{w_{1,-2}}{x^2} + \ldots + \frac{w_{1,-q}}{x^q} \right) y, \quad (11)$$

  for some positive integers p and q.
  Imposing the regularity of this expression at the singular point requires the vanishing of $w_{0,k}$, $k = -1, -2, \ldots$, and of $w_{1,k}$, $k \neq -1$. Thus v has to be proportional to y/x. This leads us to our second guess for β_1, namely $\beta_1 = y/x$. We now repeat the above. With this new guess we find that v cannot have a polynomial part in x, nor a part that is linear in y and at worst has a first-order pole at $x = 0$. As a result, the set V is empty, and we conclude that $\beta_1 = y/x$.
- Our first guess for β_2 is $\beta_2 = y^2$ and the set V consists of all elements $v = w_0(x) + w_1(x)y + w_2(x)y^2$, modulo polynomials in x, multiplied by 1, y/x or y^2. Again using a Laurent series approach and imposing regularity at the places P_1 and P_2 we find that v is of the form $v = w_{2,-1}y^2/x + w_{2,-2}y^2/x^2 + w_{2,-3}y^2/x^3$. Several choices are possible. If we make the worst choice (*i.e.*, the choice leading to the longest iteration) and make our new guess $\beta_2 = y^2/x$, we repeat this loop, only to conclude that the new set V contains elements of the form $w_{2,-2}y^2/x^2 + w_{2,-3}y^2/x^3$, a few more iterations lead us to our final guess: $\beta_2 = y^2/x^3$. With this guess we determine the set V to be empty.
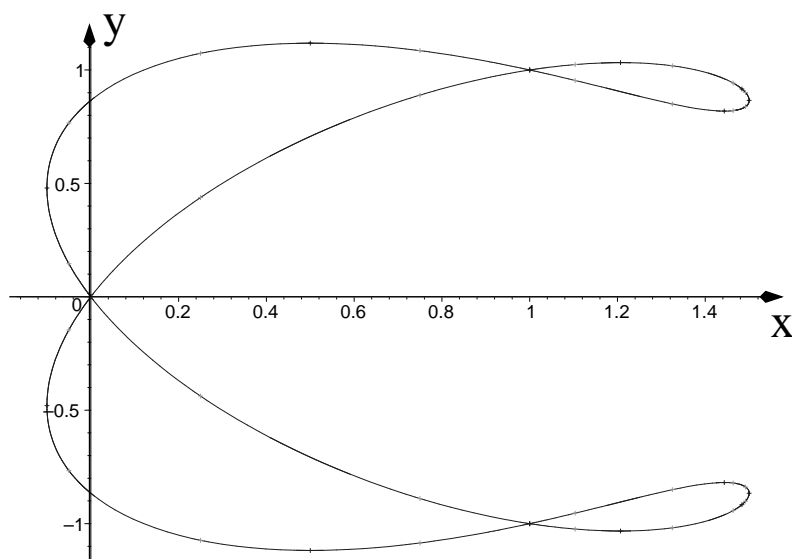
Fig. 2. The real graph of the Ampersand curve.

This concludes the construction of the integral basis for this example. As a last check, we verify explicitly that y/x and y^2/x^3 satisfy monic polynomial equations with coefficients that are polynomials in x and y. Indeed:

$$\left(\frac{y}{x}\right)^3 + 2x\left(\frac{y}{x}\right) - x^4 = 0, \quad \left(\frac{y^2}{x^3}\right)^2 + 2\left(\frac{y^2}{x^3}\right) - xy = 0. \tag{12}$$

The command `integral_basis` calculates this integral basis immediately:

```
># load the algcurves package
>with(algcurves):
># define the algebraic curve
>f:=y^3-x^7+2*x^3*y:
># calculate an integral basis for f(x,y)=0
>integral_basis(f,x,y);
```

$$\left[1, \frac{y}{x}, \frac{y^2}{x^3}\right]$$

Example. Consider the algebraic curve defined by

$$f(x,y) = (y^2 - x^2)(x-1)(2x-3) - 4(x^2 + y^2 - 2x)^2 = 0. \qquad (13)$$

This curve is known as the Ampersand curve. Its graph for $(x,y) \in \mathbb{R}^2$ is shown in Fig. 2. The figure was produced using the `plot_real_curve` command of the "algcurves" package. The curve has three finite singular points: at $(x,y) = (0,0)$, $(1,1)$ and $(1,-1)$, all double points. The Puiseux expansions specifying the places at these points are:

$$(0,0): \begin{cases} P_1 : (x = t, y = t\sqrt{19/3} + \ldots), \\ P_2 : (x = t, y = -t\sqrt{19/3} + \ldots), \end{cases} \qquad (14)$$

$$(1,1): \begin{cases} P_3 : (x = 1 + t, y = 1 + t(\sqrt{33} - 1)/16 + \ldots), \\ P_4 : (x = 1 + t, y = 1 - t(\sqrt{33} + 1)/16 + \ldots), \end{cases} \qquad (15)$$

$$(1,-1): \begin{cases} P_5 : (x = 1 + t, y = -1 + t(\sqrt{33} + 1)/16 + \ldots), \\ P_6 : (x = 1 + t, y = -1 - t(\sqrt{33} - 1)/16 + \ldots). \end{cases} \qquad (16)$$

It should be noted that with $x = 0$ there are two more regular places, which play a role in the following calculation of the integral basis of (13).

- We start with $\beta_0 = 1$.
- Our first guess for β_1 is $\beta_1 = y\beta_0 = y$. With this guess, the set V consists of all elements $v = w_0(x) + w_1(x)y$ without any polynomial parts of first degree in y. Since we are interested in the behavior at the origin and at the singular points with $x = 1$, we represent v using a partial fraction decomposition as

$$v = \frac{v_{0,-1}}{x} + \frac{v_{0,-2}}{x^2} + \ldots + \frac{w_{0,-1}}{x-1} + \frac{w_{0,-2}}{(x-1)^2} + \ldots +$$
$$\left(\frac{v_{1,-1}}{x} + \frac{v_{1,-2}}{x^2} + \ldots + \frac{w_{1,-1}}{x-1} + \frac{w_{1,-2}}{(x-1)^2} + \ldots \right) y. \qquad (17)$$

Here, and in the rest of this example, the $\ldots$ denote that more terms may appear, but up to a finite number. Imposing the regularity of this expression at the two regular places with $x = 0$ enforces $v_{j,k} = 0$, for all choices of j and k. Next, imposing the regularity of the remaining expression at P_3 to P_6 imposes too many conditions, resulting in all coefficients being equated to zero. Thus $\beta_1 = y$.

- Our first guess for β_2 is $\beta_2 = y^2$ and the set V consists of all elements $v = w_0(x) + w_1(x)y + w_2(x)y^2$, modulo polynomials in x, multiplied by 1, y or y^2. Again using a partial fraction approach we write

$$v = \frac{v_{0,-1}}{x} + \frac{v_{0,-2}}{x^2} + \ldots + \frac{w_{0,-1}}{x-1} + \frac{w_{0,-2}}{(x-1)^2} + \ldots +$$

$$\left(\frac{v_{1,-1}}{x} + \frac{v_{1,-2}}{x^2} + \ldots + \frac{w_{1,-1}}{x-1} + \frac{w_{1,-2}}{(x-1)^2} + \ldots \right) y +$$

$$\left(\frac{v_{2,-1}}{x} + \frac{v_{2,-2}}{x^2} + \ldots + \frac{w_{2,-1}}{x-1} + \frac{w_{2,-2}}{(x-1)^2} + \ldots \right) y^2. \qquad (18)$$

We first impose the conditions originating from the singular and regular points corresponding to $x = 0$. These only affect the coefficients $v_{j,k}$. From the Puiseux series P_1 and P_2, it follows immediately that $v_{j,k} = 0$ for $k < -2$. The remaining $v_{j,k}$ all vanish to ensure the regularity of v at the regular points at $x = 0$. Thus, at this stage the most general element of V might be of the form

$$v = \frac{w_{0,-1}}{x-1} + \frac{w_{0,-2}}{(x-1)^2} + \ldots + \left(\frac{w_{1,-1}}{x-1} + \frac{w_{1,-2}}{(x-1)^2} + \ldots \right) y +$$

$$\left(\frac{w_{2,-1}}{x-1} + \frac{w_{2,-2}}{(x-1)^2} + \ldots \right) y^2. \qquad (19)$$

Imposing the conditions from the places P_3, ..., P_6, note that all denominators in (19) are powers of t. Using the zeroth order Puiseux expansions at these places, we find that v reduces to

$$v = \frac{y^2 - 1}{x - 1} \left(w_{2,-1} + \frac{w_{2,-2}}{x-1} + \frac{w_{2,-3}}{(x-1)^2} + \ldots \right). \qquad (20)$$

Lastly, all coefficients $w_{2,k}$ vanish for $k \neq -1$ as there are no numerators left to cancel their singularity. Thus,

$$v = w_{2,-1} \frac{y^2 - 1}{x - 1}, \qquad (21)$$

and we are led to choose $\beta_2 = (y^2 - 1)/(x - 1)$. With this choice, we determine the new set V to be empty. Thus we have determined the third element of the integral basis.

- To find the final element of the integral basis for (13), we initially guess $\beta_3 = y^3$. A similar, but lengthier, calculation to the above results in

$$v = v_{3,-1} \frac{y(y^2 - 3/4)}{x} + \frac{y^2 - 1}{x - 1} (w_{3,-1} y + w_{2,-1}). \qquad (22)$$

To choose a new representative for β_3, we impose (8), which leads to the choice

$$\beta_3 = \frac{4y^3 - xy - 3}{4x(x - 1)}. \qquad (23)$$

With this choice the new set V is found to be empty, thus we have finished the determination of the integral basis of (13).

The command `integral_basis` agrees with our calculation of the integral basis:

```
># load the algcurves package
>with(algcurves):
># define the algebraic curve
>f:=(y^2-x^2)*(x-1)*(2*x-3)-4*(x^2+y^2-2*x)^2:
># calculate an integral basis for f(x,y)=0
>integral_basis(f,x,y);
```

$$\left[1, y, \frac{-1+y^2}{-1+x}, \frac{y^3}{(-1+x)x} - \frac{y(x+3)}{4(-1+x)x} \right]$$

A few simple algebraic manipulations confirm this integral basis to be identical to the one constructed for this example above.

5 Singularities of a Plane Algebraic Curve

The singularities of a plane algebraic curve are those points that prevent us from identifying the compactified algebraic curve with a Riemann surface. In order to obtain a Riemann surface from a plane algebraic curve, these singularities need to be resolved. There are various ways of doing this. A popular way (e.g. [Abh90]) is the use of quadratic transformations, to essentially unravel the behavior at the singular points by adding extra dimensions. Our approach is different. As discussed in Section 3, we employ Puiseux series. These do not allow us to unravel the behavior at the singular points, but they do allow us to determine how to pass through singular points. In topological terms, they determine a coordinate chart of the singular point, with which a coordinate atlas may be built, leading to the manifold structure required for a Riemann surface.

Computing the singularities

Let us consider finite singularities first. We will remark on singularities at infinity at the end of this section. Let $R(x)$ be the resultant of $f(x,y)$ and $\partial_y f(x,y)$ [Gri89]. In other words,

$$R(x) = \tag{24}$$

$$\det \begin{pmatrix} a_n & a_{n-1} & \ldots & a_1 & a_0 & 0 & \ldots & 0 \\ 0 & a_n & a_{n-1} & \ldots & a_1 & a_0 & & \ldots & 0 \\ \vdots & \ddots & & & & & \ddots & \vdots \\ 0 & \ldots & a_n & a_{n-1} & \ldots & & a_1 & a_0 & 0 \\ 0 & \ldots & 0 & a_n & a_{n-1} & \ldots & & a_1 & a_0 \\ na_n & (n-1)a_{n-1} & \ldots & a_1 & 0 & \ldots & & 0 & 0 \\ 0 & na_n & (n-1)a_{n-1} & \ldots & a_1 & & 0 & \ldots & 0 \\ \vdots & \ddots & & & & & & \ddots & \vdots \\ 0 & \ldots & 0 & na_n & (n-1)a_{n-1} & \ldots & & a_1 & 0 \\ 0 & 0 & \ldots & 0 & na_n & (n-1)a_{n-1} & \ldots & a_1 \end{pmatrix}.$$

Here all the coefficients a_k, $k = 0, \ldots, n$, are as in (1), thus they are functions of x. The roots of $R(x)$ are the x-coordinates of the places that satisfy

$$f(x, y) = 0, \quad \partial_y f(x, y) = 0. \tag{25}$$

Since singularities correspond to more than one place on the Riemann surface, we seek the roots of $R(x)$ that have multiplicity 2 or higher. Let $S = (x_1, \ldots, x_s)$ be the list of these roots. For each $x_k \in S$, we solve

$$f(x_k, y) = 0. \tag{26}$$

Denote the solutions of this equation by $(y_{k1}, \ldots, y_{kn})$ (some entries may be repeated). This results in a number of places (x_k, y_{kj}), $k = 1, \ldots, s$, $j = 1, \ldots, n$. Those places that satisfy

$$\partial_x f(x_k, y_{kj}) = 0, \quad k = 1, \ldots, s, \quad j = 1, \ldots, n, \tag{27}$$

are singular points of the algebraic curve specified by (1). Using homogeneous coordinates, these points are denoted $(x_k, y_{kj}, 1)$.

For singular points at infinity, we proceed as follows. The points at infinity are found by solving the homogeneous polynomial equation (3) of degree d

$$F(X, Y, 0) = 0 = X^d F(1, Y/X, 0) = Y^d F(X/Y, 1, 0). \tag{28}$$

This results in d points, possibly repeated, written in homogeneous coordinates as $(X_j, Y_j, 0)$, $j = 1, \ldots, d$. Those points that satisfy

$$F_X(X, Y, Z) = F_Y(X, Y, Z) = F_Z(X, Y, Z) = 0, \tag{29}$$

are singular points. Incorporating the newly found singular points at infinity, we denote the set of all singular points as

$$\mathcal{S} = \{P_1, \ldots, P_S\}, \tag{30}$$

where S denotes the number of distinct singularities of the algebraic curve.

Each singularity on an algebraic curve is categorized by three numbers: m, δ, and R: its multiplicity, its delta invariant and its number of local branches, respectively. In rough terms, for a point P on the algebraic curve, m is the number of tangent lines at P (counting a tangent line as many times as its multiplicity), δ is the number of ordinary double points that coalesce to form the singularity at P, and R is the number of local branches that emanate from P. A common approach [BK86, Abh90, Wal62] is to compute these numbers by employing successive quadratic transformations $(x, y) \mapsto (x, yx)$ to "blow up" or resolve singularities into "infinitely near" but distinguishable curve components. Instead, the algorithms of the "algcurves" package use Puiseux expansions to compute m, δ and R.

Note that triples (X, Y, Z) corresponding to places at infinity may be brought to the origin by an appropriate transformation [Abh90], so it suffices to discuss the computation of m, δ and R for affine triples $(\alpha, \beta, 1)$ which are well defined by the pair (α, β). Further, using $x \mapsto x - \alpha$, all affine places corresponding to (α, β) are brought to places $(0, \beta)$ over $x = 0$. In the descriptions below, we assume such transformations have been executed, to simplify the discussion.

Branching number of a singularity

The number R of local branches at $(0, \beta)$ is computed by computing all the Puiseux expansions over $x = 0$, and counting how many of them have y-value β at the center. In other words, $R = \sum_j |r_j|$, where the sum runs over all places at the singular point.

Multiplicity of a singularity

The multiplicity of a place $P = (0, \beta)$ on the plane algebraic curve defined by $f(x, y) = 0$ is the number of (complex) tangent lines that meet there once multiple tangencies are properly counted [Gri89].

Over a regular point $x = \alpha$ there are n distinct y-values, each yielding a distinct pair (α, β_j). Thus the multiplicity of a pair (α, β_j) over a regular point α is necessarily one. Over a singular point, sets of the n branches of the algebraic cover coalesce at least one of the β_j. Suppose that some number, say ℓ, of branches all coalesce at $(\alpha = 0, \beta)$. Then the multiplicity of $(\alpha = 0, \beta)$ (and thus that of the homogeneous triple $(\alpha = 0, \beta, 1)$ is the sum of the multiplicities of each of the ℓ branches. The multiplicity of each branch is calculated from the Puiseux expansions whose centers are $(\alpha = 0, \beta)$: define the lines $L(x, y) = a(x - \alpha) + b(y - \beta) = 0$, with $a, b \in \mathbb{C}$. To properly count the tangencies at place $P = (t^r, \beta + \beta' t^s + \cdots)$ with center $(\alpha = 0, \beta)$, we calculate the valuation of $L(t^r, \beta' t^s + \cdots)$ (i.e., the exponent of the lowest power of t in $L(t^r, \beta' t^s + \cdots)$) and minimize it over all a and b [Wal62].

One may see that the multiplicity of $P = (t^r, \beta + \beta' t^s + \cdots)$ is the minimum of r and s. Indeed, we calculate the minimum intersection multiplicity of

expansion P with lines through $(0, \beta)$ given by (i) $x = 0$ and (ii) $y = \beta$. (i) First, any line of the form $ax = 0$ (or, L with $a \neq 0$, $b = 0$) evaluated at P_i results in $at^r = 0$. Thus the valuation of $L(x, y) = 0$ is r for any value of $a \neq 0$. (ii) Next, any line for which $b \neq 0$, when intersected with P, is given by $L = at^r + b(\beta + \beta' t^s + \cdots - \beta) = at^r + b(\beta' t^s + \cdots) = 0$. If $r \leq s$, then the valuation is r. Otherwise, the valuation is s.

Delta invariant of a singularity

A singular point is said to be an *ordinary singular point* if all the branches at this point intersect transversely (*i.e., the tangent lines at the point to all these branches are all distinct*). The delta invariant δ of an ordinary k-tuple center (α, β) is the number of transverse intersections that occur there. For instance, 4 lines crossing transversely at (α, β) may be "perturbed" slightly to create a situation with $4(4 - 1)/2$ intersections, each a transverse intersection of two lines. The delta invariant of any ordinary k-tuple singularity (α, β) is the number $\delta = m(m - 1)/2$, where m is the multiplicity of the center (α, β).

Suppose the branches do not cross transversely at (α, β), in other words (α, β) is not an ordinary k-tuple center. Then δ is instead defined to be the number of linear conditions imposed by the Puiseux expansions with center (α, β) on the construction of the integral basis of Sect. 4, but without incorporating the singularities not at (α, β). This definition encompasses the one above, which only holds for ordinary k-tuple centers.

The "algcurves" command `singularities` uses a formula which allows for the computation of the delta invariant directly in terms of the quantities associated with the Puiseux series at the singular point (see, for instance, [**?**]).

To explain the formula used to compute the delta invariant δ of the center $(0, \beta)$, it is necessary to introduce the intersection Int_P of Puiseux expansion P. Suppose all the places with center $(0, \beta)$ are given by $P_1, \ldots, P_m$, and let r_j be the branching number of P_j. Further, suppose $\hat{y}_j(x)$ is a series in powers of the local coordinate x^{1/r_j}, each with constant term β. Recall that upon conjugation using the r_j-th roots of unity, $\hat{y}_j$ accounts for r_j y-roots of $F = 0$. Thus, near $x = 0$, F may be factored as

$$f = \Pi_{j=1}^m \Pi_{k=1}^{r_j} \left(y - \hat{y}_j(e^{2i\pi k/r_j} x) \right) * \Pi_{j=m+1}^n (y - \hat{y}_j(x)), \qquad (31)$$

where $\hat{y}_j(0) \neq \beta$ for $m + 1 < j \leq n$. Rewriting (31) more simply as a product of n factors, without regard to the places from which those factors arose, we have

$$f = \Pi_{k=1}^n (y - \widetilde{y}_k(x)). \qquad (32)$$

The intersection index Int_{P_j} of place P_j is then given by

$$\mathrm{Int}_{P_j} = \sum_{k=1,\, k \neq j}^n \mathrm{ord}_x(\hat{y}_j(x) - \widetilde{y}_k(x)), \qquad (33)$$

where $\text{ord}_x(g(x))$ denotes the lowest, possibly fractional, exponent of x appearing in $g(x)$. The delta invariant of the center $(0, \beta)$ is then given by

$$\delta_{(0,\beta)} = \sum_{j=1}^{m} \frac{r_j \text{Int}_{P_j} - r_j + 1}{2}. \tag{34}$$

Example. Recall from Section 3 that the ramphoid cusp given by $f = (x^2 - x + 1)y^2 - 2x^2 y + x^4 = 0$ is described near $x = 0$ by the single Puiseux series $y = x^2 + x^{5/2} + \cdots$. To recover both roots of $f = 0$, we conjugate over the square roots of unity. Thus, near $x = 0$, f may be factored as

$$f = (y - x^2 - x^{5/2} + \cdots)(y - x^2 + x^{5/2} + \cdots). \tag{35}$$

Int_P is the lowest exponent in x appearing in the expression obtained by substituting $y = x^2 + x^{5/2} + \cdots$ into the right-hand factor in (35):

$$\text{Int}_P = \text{ord}_x(x^2 + x^{5/2} + \cdots - x^2 + x^{5/2} + \cdots) = 5/2.$$

Noting there is only one place over $x = 0$, and the branching number there is 2, the delta invariant of the center $(0,0)$ is, by (34), $((5/2)2 - 2 + 1)/2 = 2$.

Example. Consider the plane algebraic curve defined by $f = y^3 - x^7 + 2x^3 y = 0$. The Puiseux expansions over $x = 0$ are

$$\bar{y}_1 = x^4/2 + \cdots, \quad \bar{y}_2 = -i\sqrt{2}x^{3/2} - x^4/4 + \cdots,$$

thus, near $x = 0$, F may be factored as

$$\left(y - x^4/2 + \cdots\right)\left(y + i\sqrt{2}x^{3/2} + 2x^4 + \cdots\right)\left(y + \sqrt{2}x^{3/2} + 2x^4 + \cdots\right). \tag{36}$$

First we calculate the contribution to (34) from $\hat{y}_1$. The branching number in this case is $r_1 = 1$. The quantity Int_{P_1} is the order in x of

$$\left(x^4/2 + \cdots + i\sqrt{2}x^{3/2} + 2x^4 + \cdots\right)\left(x^4/2 + \cdots + \sqrt{2}x^{3/2} + 2x^4 + \cdots\right),$$

which is $3/2 + 3/2 = 3$. Therefore the contribution to $\delta_{(0,0)}$ from $\hat{y}_1$ is $((1)(3) - 1 + 1)/2 = 3/2$. Next, we calculate the contribution from $\hat{y}_2$. The branching number in this case is 2, and Int_2 is the lowest exponent in x in the result of substituting $y = \hat{y}_2$ into the first and third factors of (36):

$$\text{Int}_{P_2} = \text{ord}_x \left(\left(-i\sqrt{2}x^{3/2} - x^4/4 + \cdots - x^4/2 + \cdots \right) * \cdots \right.$$
$$\left. \cdots * \left(-i\sqrt{2}x^{3/2} - x^4/4 + \cdots + \sqrt{2}x^{3/2} + 2x^4 - \cdots \right) \right)$$
$$= 3$$

Thus the contribution due to $\hat{y}_2$ is $((2)(3) - 2 + 1)/2 = 5/2$, and $\delta_{(0,0)} = 3/2 + 5/2 = 4$.

Next we present a few examples of the use of the `singularities` command of the "algcurves" package to calculate with singularities of plane algebraic curves. We restrict the coefficients of the polynomials in the examples to be integers to keep the output relatively simple. The Maple implementation is in no way restricted to such curves.

The output of the command `singularities` is a set of lists, one list for each singularity. Each list consists of the homogeneous coordinates representation of the singularity P, followed by, in order, the multiplicity m, the delta invariant δ and the number of local branches R at P. The procedure computes all singularities up to conjugation. Thus if a singularity $[\text{RootOf}(\_Z^2 - 2), 1, 1]$ is present in the output, and if $\text{RootOf}(\_Z^2 - 2)$ does not appear as a coefficient in the curve, then $[-\text{RootOf}(\_Z^2 - 2), 1, 1]$ is a singular point as well but is suppressed in the output. Here we have adopted the Maple notation $\text{RootOf}(\_Z^2 - 2)$ to denote the Z-roots of the equation $Z^2 - 2$. In other words, $\text{RootOf}(\_Z^2 - 2)$ is a placeholder for both $\sqrt{2}$ and $-\sqrt{2}$.

Example. The curve $f = y^2 + x^3 - x^2 = 0$ has a node, that is an ordinary double point, at the origin and a branch point at $x = 1$. Figure 3 shows the real graph of $f(x, y) = 0$. In this example we compute m, δ and R for the singularity at $(0, 0)$ (or in homogeneous coordinates, $(0 : 0 : 1)$). First, we calculate the Puiseux expansions over $x = 0$.

```
># read in the package
>with(algcurves):
># define the algebraic curve
>f:=y^2+x^3-x^2:
># compute the Puiseux expansions over x=0
>puiseux(f,x=0,y,0,t);
```

$$\{[x = t, y = -t], [x = t, y = t]\}$$

There are two expansions over $x = 0$, both with center $(0, 0)$: therefore $R = 2$. Consider the first expansion. The exponent of t for the x-series is one, as is the lowest exponent for the y-series. The minimum of these two exponents is one, thus the multiplicity of the first expansion is one. A similar argument with the second expansion gives that its multiplicity is also one, resulting in a total multiplicity for the singularity of $m = 2$. The two branches cross
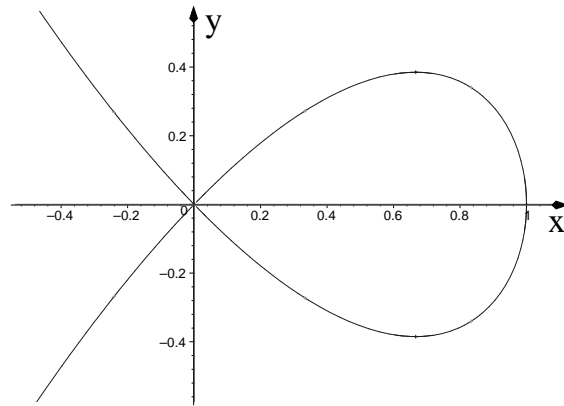
Fig. 3. The real part of the graph of $y^2 + x^3 - x^2 = 0$ displays an ordinary double point, also known as a node, at the origin. The figure was produced using the `plot_real_curve` command.

transversely, thus $(0,0)$ is an ordinary double point with delta invariant given by $\delta = 2(2-1)/2 = 1$. We confirm this using the command `singularities`.

```
>singularities(f,x,y);
```

$$\{[[0,0,1], 2, 1, 2]\}$$

Thus the origin is a singular point with multiplicity $m = 2$, delta invariant $\delta = 1$ and branching number $R = 2$.

Example. The real graph of the algebraic curve defined by

$$\begin{aligned} f &= y^6 + 3x^2y^4 - y^3 + 3x^4y^2 + 3x^2y + x^6 \\ &= (x^2 + y^2)^3 + 3x^2y - y^3 \end{aligned} \tag{37}$$

is a trefoil whose lobes meet at the origin, as shown in Fig. 4. As before, we compute the Puiseux series over $x = 0$ and, using these expansions, explain the output of the command `singularities`.

```
># define the algebraic curve
>f:=(x^2 +y^2)^3 + 3x^2y - y^3:
># compute the Puiseux expansions over x=0
>puiseux(f,x=0,y,0,t);
```
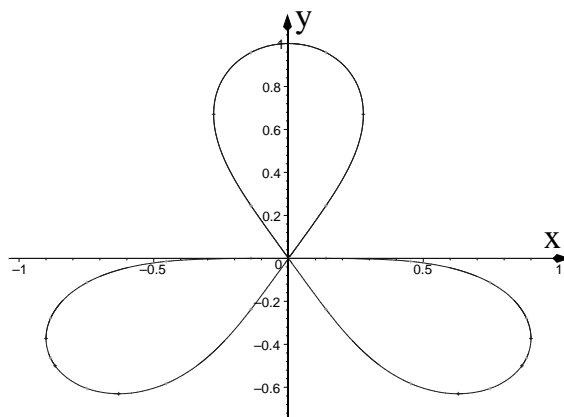
Fig. 4. The real part of the graph of $(x^2+y^2)^3+3x^2y-y^3 = 0$ shows the presence of a singularity at the origin which is an ordinary triple point. The figure was produced using the `plot_real_curve` command.

$$\{[x = t, y = \text{RootOf}(\_Z^2 + \_Z + 1)], [x = t, y = t\,\text{RootOf}(\_Z^2 - 3)],$$
$$[x = t, y = 0], [x = t, y = 1]\}$$

Note that the first and last expansions in the set above do not have center at the origin. Further, as explained above, the expansion $[x = t, y = t\,\text{RootOf}(\_Z^2-3)]$ represents two places (that is $(t, \sqrt{3}t+\cdots)$ and $(t, -\sqrt{3}t+\cdots)$), each with the same center (namely $(0,0)$). Thus there are three local expansions with center $(0,0)$. As the three branches have distinct slopes, the origin is an ordinary triple point. Thus its delta invariant is $3(2)/2 = 3$.

```
>singularities(f,x,y);
```

$$[[\text{RootOf}(\_Z^2 + 1), 1, 0], 3, 3, 3], [[0, 0, 1], 3, 3, 3]$$

As the singularities are computed up to conjugation, the first triple in the set above represents the two (non-affine) homogeneous triples $(i : 1 : 0)$ and $(-i : 1 : 0)$, each having the same values for m, δ and R. The sum of the delta invariants is 9 and not 6 as might be expected from the above output.

6 Genus of a Riemann Surface

In this section, we discuss how one algorithmically computes the genus of a Riemann surface associated with a possibly singular plane algebraic curve. The algorithm relies on the various quantities discussed in the previous sections. The genus is an important ingredient for the algorithms of the following sections on the computation of the Riemann matrix (Section 10) and the Abel transform (Section 11).

Once the delta invariants of all singularities (finite and infinite) are known, the genus is given by $(d-1)(d-2)/2$ minus the sum of all the delta invariants [Abh90]:

$$g = \frac{(d-1)(d-2)}{2} - \sum_{P \in \mathcal{S}} \delta_P. \tag{38}$$

Example. In what follows, a few examples of the output of the `genus` command are given. If the polynomial given as input can be factored, the `genus` command returns -1. We consider two algebraic curves defined by $f_j(x,y) = 0$, $j = 1,2$:

$$f_1 = y^4 - y^2 x + x^2, \tag{39}$$
$$f_2 = y^3 - (x^3 + y)^2 + 1. \tag{40}$$

The first of these curves, $f_1(x,y) = 0$ is reducible. The second one is a curve of genus 4.

```
># load the algcurves package
>with(algcurves):
># define the algebraic curve
>f1:=y^4-y^2 x+x^2:
># calculate the genus of f1(x,y)=0
>genus(f1,x,y);
>Warning, negative genus so the curve is reducible
```

$$-1$$

```
># factor the curve
>evala(AFactor(f1));
```

$$\left(y^2 + \frac{-1 - \text{RootOf}(\_Z^2 + 3)}{2}x\right)\left(y^2 + \frac{-1 + \text{RootOf}(\_Z^2 + 3)}{2}x\right)$$

```
># define the algebraic curve
>f2:=y^3-(x^3+y)^2+1:
># calculate the genus of f2(x,y)=0
>genus(f2,x,y);
```

4

```
># the same result is obtained if we switch the order of
># the variables
>genus(f2,y,x);
```

4

7 Monodromy of a Plane Algebraic Curve

The monodromy of a plane algebraic curve is the input for Tretkoff & Tretkoff's algorithm [TT84] for the construction of a homology basis of a Riemann surface, as discussed in Section 8. In this section we discuss an algorithm to compute the monodromy of a plane algebraic curve in its own right.

An algebraic curve gives rise to a covering of the Riemann sphere[2]. The monodromy of a plane algebraic curve encodes how the different sheets of this covering glue together to form one smooth whole: starting near one of the branch points $x = b$, we label the sheets of the algebraic covering $y(x)$ with labels $1, 2, \ldots, n$. When $y(x)$ is analytically continued counterclockwise around the branch point $x = b$, the sheets will be interchanged, and a permutation σ_b acts accordingly on these sheet labels. The collection of the permutations at all branch points (including any singular branch points and points at infinity) determines the monodromy group of the algebraic curve (1). More background on the monodromy group is found in [DFN85], whereas [TT84] provides more details that are useful for the later use of the monodromy of a plane algebraic curve in computing the homology of the associated Riemann surface.

The calculation of the monodromy group of an algebraic covering $y(x)$ requires several ingredients. First, we select a *base point* $x = a$ in the complex x-plane. This base point is a finite regular point of the algebraic covering $y(x)$, i.e., for $x = a$, n distinct finite y-values exist. These n y-values may be assigned an order, $(y_1, y_2, \ldots, y_n)$. This ordering of the n y-values labels the sheets of the algebraic covering $y(x)$. For each branch point b one chooses a path γ_b in the complex x-plane which starts and ends at $x = a$ and encircles only the branch point $x = b$, counterclockwise. Next, the n-tuple $(y_1, y_2, \ldots, y_n)$ is analytically continued around this path γ_b. When one returns to $x = a$, a new n-tuple is found, which has the same entries as $(y_1, y_2, \ldots, y_n)$, but reshuffled: $(y_{\sigma_b(1)}, y_{\sigma_b(2)}, \ldots, y_{\sigma_b(n)})$. The permutation σ_b is read off from this reshuffled vector.

We now discuss the steps of this procedure more systematically.

1. **The problem points of the analytic continuation:**

---

[2] In fact, Riemann introduced the concept of a Riemann surface to examine this multivaluedness [Rie90]

The algebraic curve (1) defines an n-sheeted algebraic covering $y(x)$ of the extended complex x-plane. For all but a finite number of values of x in the extended complex plane $\mathbb{C}\bigcup\{\infty\}$ there are n values for $y(x)$ in $\mathbb{C}\bigcup\{\infty\}$. A value for x corresponds to a singularity or a *branch point* if and only if there are fewer than n values for $y(x)$. A branch point of this n-sheeted covering is defined as an x-value $x = b$ where $y(x)$ does not return to its original value when one analytically continues $y(x)$ once along a small circle around $x = b$.

The notion of problem points $P = \{b_1, b_2, \ldots, b_m\}$ was introduced in [DvH01] for the purpose of singling out the finite x-values corresponding to those places on the algebraic curve that require special treatment for the purposes of numerical analytic continuation. The problem points contain the collected x-values giving rise to singular points, branch points and points for which $y = \infty$. In short, the problem points are all finite x-values for which the equation $f(x, y) = 0$ gives rise to fewer than n finite and distinct roots y.

The set of problem points is found by calculating (i) the roots of $\Delta(x) = 0$, where $\Delta(x)$ is the discriminant of $f(x, y)$, namely the resultant of $f(x, y)$ and $f_y(x, y)$ divided by $a_n(x)$ [vdW91], and (ii) the roots of $a_n(x) = 0$. If x is a root of the latter equation, then the equation $f(x, y) = 0$ effectively drops in degree, resulting in some roots y being infinite. Note that the addition of the roots of $a_n(x) = 0$ is necessary due to the definition of the discriminant. Since both the discriminant $\Delta(x)$ and $a_n(x)$ are polynomials in x, the number of problem points is finite. All branch points of our algebraic covering are discriminant points, but not all discriminant points are branch points. Discriminant points which are not branch points are singular points. Note that discriminant points which are branch points may also be singular. In the algorithms, the problem points are the union of roots of $a_n(x) = 0$ or $\Delta(x) = 0$.

In principle, only the knowledge of the positions of the branch points is required for the purposes of computing the permutations. However, to avoid numerical problems during the analytical continuation of $(y_1, y_2, \ldots, y_n)$, the other problem points, such as singularities, are avoided as well. The monodromy algorithm treats them on the same footing as the branch points, although they are removed from the final output, since their permutations σ_b are all equal to the identity. Lastly, although the point $x = \infty$ is not included in the set of problem points, it is also avoided.

2. **Encircling the problem points:** In order to compute the monodromies of the algebraic covering $y(x)$, the vector $y(x)$ is analytically continued along paths encircling the problem points. In order to simplify control of the numerical accuracy, the paths stay a distance $r(b_i)$ away from each problem point b_i. Thus, with every problem point b_i, we associate a radius $r(b_i)$ as follows:

$$r(b_i) = \frac{2}{5}\rho(b_i, \{b_1, b_2, \ldots, b_m\}\setminus\{b_i\}), \tag{41}$$

where ρ denotes distance. In other words, $r(b_i)$ is two fifths of the distance of b_i to the next-nearest problem point. The ratio $2/5$ is somewhat arbitrary; other numbers between 0 and $1/2$ might be used. Important is that the circles $C(b_i, r(b_i))$ do not intersect each other.

3. **The choice of the base point:** Now a base point a is chosen, such that $x = a$ is at least a distance $r(b_s)$ away from the nearest problem point b_s, and such that the real part of a is smaller than the real parts of any of the b_i. By the latter choice, the arguments of $b_i - a$ are between $-\pi/2$ and $\pi/2$. For plane algebraic curves defined by (1) with real coefficients, the base point is chosen to be real.

4. **Labeling of the sheets:** At the base point $x = a$ there are n distinct finite y-values, by construction. These are determined numerically as the solutions of $f(a, y) = 0$. Let these n y-values be assigned an order $(y_1, y_2, \ldots, y_n)$, which is denoted as $\boldsymbol{y}(a)$. Assigning such an order to these y-values labels the sheets of the algebraic covering $y(x)$: sheet one is the sheet containing y_1, sheet 2 is the sheet containing y_2, and so on. Note that because $x = a$ is at least a distance $r(b_s)$ away from the nearest problem point b_s, the values $(y_1, y_2, \ldots, y_n)$ are well separated.

5. **Ordering the problem points of the analytic continuation:** A consistent ordering needs to be imposed on the problem points. We choose to order these points according to their argument with respect to the base point: if $\arg(b_i - a) < \arg(b_j - a)$, then b_i precedes b_j in the ordering, where $\arg(\cdot)$ denotes the argument function. If $\arg(b_i - a) = \arg(b_j - a)$, then b_i precedes b_j in the ordering if $|b_i - a| < |b_j - a|$. This ordering results in an ordered m-tuple of problem points: $(b_1, b_2, \ldots, b_m)$. The same notation is used for the ordered problem points as for the elements of the non-ordered set.

6. **Choice of the paths:** Next, we choose paths for the analytic continuation. These paths are composed of line segments and semi-circles. The simplest path $L(b_i)$ around b_i consists of one line segment from a to $b_i - r(b_i)$. This is followed by the circle $C(b_i, r(b_i))$, starting at $b_i - r(b_i)$. Successively, a line segment is followed from $b_i - r(b_i)$, back to a. However, if this path intersects one of the circles $C(b_j, r(b_j))$, $j \neq i$, we modify the path to another one that is homotopic[3] to it. If a path intersects one of the circles $C(b_j, r(b_j))$, $j \neq i$, this indicates that it comes close to the problem point b_j. As a consequence, the sheets of the algebraic covering would not be well separated along the path, which complicates the numerical analytical continuation. Therefore we wish to avoid this. The situation may be remedied as indicated in Fig. 5: the path takes a detour along a semi-circle around b_j. Whether this semi-circle goes above or below b_j depends on

---

[3] In this context we call two paths homotopic to each other if they may be continuously deformed to one another without crossing any problem points
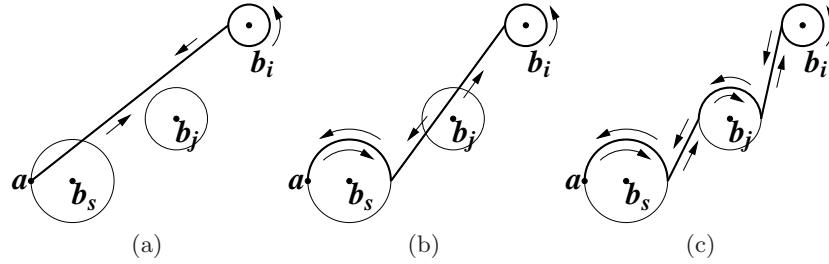
Fig. 5. Choosing the path from $x = a$ to $x = b_i$. The path around b_i is indicated in a thick black line. (a) The simplest path intersects $C(b_s, r(b_s))$. (b) This is remedied by a new path which is homotopic to the previous one. The new path intersects $C(b_j, r(b_j))$. (c) This is remedied by another path, which is homotopic to both previous paths

the relative positions of a, b_i and b_j. The semi-circle is chosen such that the new path is deformable to $L(b_i)$, without crossing any problem points of the analytic continuation.

This process is iterated, until a path is obtained, which stays at least $r(b_j)$ away from b_j, for $j = 1, 2, \ldots, m$. The iteration of this process is not sufficient to ensure that the chosen path is homotopic to the straight-line path from the base point a to $b_i - r(b_i)$. To ensure that a correct path is chosen, our implementation explicitly checks for the presence of problem points between the chosen path and the straight-line path. If such points are present, the path is modified to go around them, after which the check procedure is re-iterated.

7. **Numerical analytic continuation:** Consider two non-problem points $x = x_1$ and $x = x_2$. Corresponding to x_1 is an ordered n-tuple $\boldsymbol{y}(x_1)$. When a path is followed in the complex x-plane from x_1 to x_2, the entries of $\boldsymbol{y}(x_1)$ follow paths on the algebraic cover to the roots of $F(x_2, y) = 0$, which gives rise to an n-tuple $\boldsymbol{y}(x_2)$, whose ordering is induced by the ordering of $\boldsymbol{y}(x_1)$. If x_1 and x_2 are relatively close to each other so that the path between them deviates little from a straight-line segment and provided it does not pass through or near any problem points, then

$$\boldsymbol{y}(x_2) = \boldsymbol{y}(x_1) + \boldsymbol{y}'(x_1)(x_2 - x_1) + \vartheta(|x_2 - x_1|^2), \qquad (42)$$

and the last term is small when x_2 and x_1 are sufficiently close (to make this precise one needs to bound the second derivative of $\boldsymbol{y}(x)$ to find a bound for $\vartheta(|x_2 - x_1|^2)$). Here $\boldsymbol{y}'(x_1)$ is the n-tuple of derivatives to the algebraic curve at $\boldsymbol{y}(x_1)$. Using implicit differentiation we have

$$\boldsymbol{y}'(x_1) = -\left(\frac{F_x(x_1, y_1(x_1))}{F_y(x_1, y_1(x_1))}, \frac{F_x(x_1, y_2(x_1))}{F_y(x_1, y_2(x_1))}, \ldots, \frac{F_x(x_1, y_n(x_1))}{F_y(x_1, y_n(x_1))} \right), \quad (43)$$

where a subindex x or y denotes partial differentiation and $y_i(x_1)$, $i = 1, \ldots, n$ denotes the i-th component of $\boldsymbol{y}(x_1)$. Under the above conditions, the first two terms of (42) give a good approximation to $\boldsymbol{y}(x_2)$. Having the unordered entries of $\boldsymbol{y}(x_2)$ at our disposal and comparing them with the ordered approximation $\boldsymbol{y}(x_1) + \boldsymbol{y}'(x_1)(x_2 - x_1)$ allows us to determine the ordering of these entries, resulting in the ordered n-tuple $\boldsymbol{y}(x_2)$. Clearly, in order to avoid matching up the entries of $\boldsymbol{y}(x_2)$ with the wrong entries of the ordered approximation, the acceptable size of $|x_2 - x_1|$ depends on the absolute differences between the components of $\boldsymbol{y}(x_2)$.

If $|x_2 - x_1|$ is not small, or if the path connecting them deviates significantly from a straight-line segment, then an analytic continuation from $\boldsymbol{y}(x_1)$ to $\boldsymbol{y}(x_2)$ is obtained by iterating the above process along sufficiently small segments of the path, such that the necessary conditions above are satisfied. Note that $\boldsymbol{y}(x_2)$ is dependent on the path chosen from x_1 to x_2. For brevity of notation, this dependence is not made explicit.

8. **The monodromy group:** Consider a closed path starting from the base point $x = a$ and returning there after encircling the branch point $x = b$. After analytic continuation of $\boldsymbol{y}(a)$ along this path, the entries of $\boldsymbol{y}(a)$ are recovered, but they are shuffled by the permutation σ_b.

$$\Pi(b)\boldsymbol{y}(a) = \Pi(b)(y_1(a), y_2(a), \ldots, y_n(a)) = \left(y_{\sigma_b(1)}, y_{\sigma_b(2)}, \ldots, y_{\sigma_b(n)}\right),$$
(44)

where $\Pi(b)$ denotes the action of analytic continuation along a path encircling b, which is homotopic to a path containing the base point that encircles b and no other problem points. The collection of all σ_b generates the monodromy group of the covering, which is represented here as a subgroup of S_n, the group of permutations of $\{1, 2, \ldots, n\}$. Note that this representation depends on the choice of the labeling of the y-values at $x = a$, so it is only unique up to conjugation. More details are found in [DFN85].

This representation of the monodromy group is discrete. Because of this, it is obtained exactly, despite the numerical nature of the analytic continuation.

9. **Infinity:** The point $x = \infty$ might also be a branch point. The corresponding permutation σ_∞ is computed by encircling all problem points in a clockwise sense. On the base of the covering, this is equivalent to encircling the point at infinity in a counter-clockwise sense. If this permutation is not the identity, then the point $x = \infty$ is a branch point. Otherwise it is not.

Having found this permutation, the program performs one of many internal checks by verifying that

$$\sigma_\infty \circ \sigma_{b_m} \circ \sigma_{b_{m-1}} \circ \ldots \circ \sigma_{b_2} \circ \sigma_{b_1} = 1.$$
(45)

Since a closed path in the extended complex x-plane that encircles all branch points is homotopic to a point, analytic continuation along such a path will not permute the entries of $y(a)$. Alternatively, we could use (45) to compute σ_∞, but this eliminates a possible check. In what follows, it is always assumed that the list $b_1, b_2, \ldots, b_m$ includes $x = \infty$ if it is a branch point. In this case, σ_∞ is also assumed to be included in the permutation list $\sigma_{b_1}, \ldots, \sigma_{b_m}$.

Example. We use the above algorithm to compute a representation of the monodromy group for the algebraic covering $y(x)$ corresponding to $F(x, y) = y^3 - (x^3 + y)^2 + 1 = 0$: the command `monodromy(f,x,y)` gives a list with three elements. The first element is the choice of the base point $x = a$. The second element is $y(a)$, which is a list of $n = 3$ elements. The third element is a list of the branch points b_i with their permutations σ_{b_i}, given in disjoint cycle notation.

```
># load the algcurves package
>with(algcurves):
># define the algebraic curve
>f:=y^3-(x^3+y)^2+1:
># calculate the monodromy representation for y(x)
>m:=monodromy(f,x,y,'showpaths'):
># the base point x=a
>m[1];
```

$$-1.27297541004$$

```
># the sheets y(a)
>m[2];
```

$$[.0907534141676 - 1.99219212537i, .0907534141676 + 1.99219212537i,$$
$$.818493171665]$$

```
># the branch points with their permutations
>m[3];
```

$$[[-.573843481646 - .993926065804i, [[2,3]]],$$
$$[-1.03977417810 - .167751539921i, [[2,3]]],$$
$$[-.372303356542 - .644848329360i, [[1,2]]],$$
$$[.374609993952 - .984346622390i, [[1,3]]],$$
$$[.665164184143 - .816595082469i, [[2,3]]],$$
$$[.744606713085, [[1,2]]], [1.14768696329, [[1,3]]],$$
$$[.665164184143 + .816595082469i, [[1,3]]],$$
$$[.374609993952 + .984346622390i, [[2,3]]],$$
$$[-.372303356542 + .644848329360i, [[1,2]]],$$
$$[-1.03977417810 + .167751539921i, [[1,3]]],$$
$$[-.573843481646 + .993926065804i, [[1,3]]]]$$

Thus, starting from the ordered sheets 1, 2 and 3 above the base point $x = -0.724402557170$ (i.e., from the ordered y-values $0.0907534141676 - 1.99219212537i$, $0.0907534141676 + 1.99219212537i$, 0.818493171665), and encircling $x = 0.374609993952 - .984346622390i$, one finds that sheet 1 has become sheet 3 and sheet 3 has become sheet 1. Sheet 2 was not affected by encircling this branch point. The optional argument `showpaths` produces Fig. 6. This shows the paths followed in the complex x-plane for the analytic continuation of $y(x)$.

Remarks

- The reader should note that throughout the above procedures, no mentioning is ever made of branch cuts. Any book on complex analysis will state that the choice of branch cuts is irrelevant for many purposes. This is clear from the presentation above: branch cuts are never introduced! Branch cuts provide a recipe for performing analytic continuation, by specifying the range of the argument function. They are also often convenient means for understanding the geometry of the Riemann surface under investigation: In practice they are artificial boundaries on the Riemann surface denoting the several sheets. They loose much of their practical value when one leaves the realm of hyperelliptic surfaces. In the above, branch cuts could have been introduced as segments from the base point to the branch points.
- The construction of the paths for a general plane algebraic curve is a hard problem. Most of the algorithms discussed in this chapter rely on local analytic structures near specific points. The construction of the paths is the main part of the algorithms, where the global geometry of the curve is encoded. It is relatively easy to construct examples, where the location of the problem points is such that the iterative algorithm described above does not terminate unless the user-specified accuracy is sufficiently high. In such cases the user may get an error message making exactly this statement, asking the user to increase the accuracy and to try again.
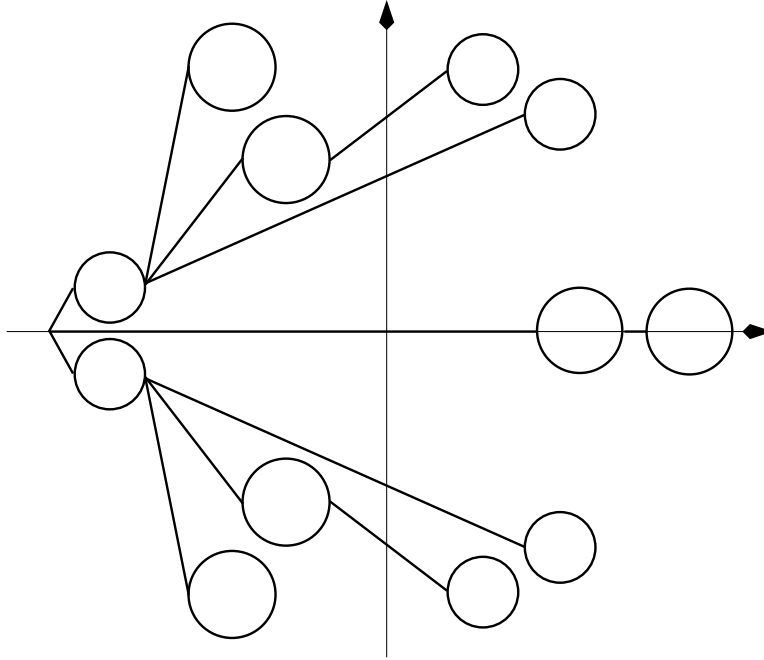
Fig. 6. The complex x-plane and the paths followed for the analytic continuation of $y(x)$, with $y^3 - (x^3 + y)^2 + 1 = 0$. The base point $x = a$ is at the left.

- Recent work by Adrien Poteaux [Pot07] has resulted in an algorithm for the computation of the monodromy of a plane algebraic curve that is verifiably correct, without requiring user interaction. The algorithm appears to be competitive in that it is computationally not significantly more expansive than that described above.

8 Homology of a Riemann Surface

With the monodromy of a plane algebraic curve at our disposal, in this section we construct a basis for the homology of the Riemann surface obtained from such an algebraic curve. We define a cycle to be a closed, oriented, smooth or piecewise smooth curve. Since a Riemann surface of genus g is topologically equivalent to a sphere with g handles, on a surface of genus > 1 there are cycles (those encircling the handles or the holes) which cannot be deformed to points. Thus such cycles are nontrivial, even if they are used as integration paths for holomorphic differentials.

Two cycles on a Riemann surface are called homotopic if they can be continuously deformed into one another. In this section, we consider the weaker
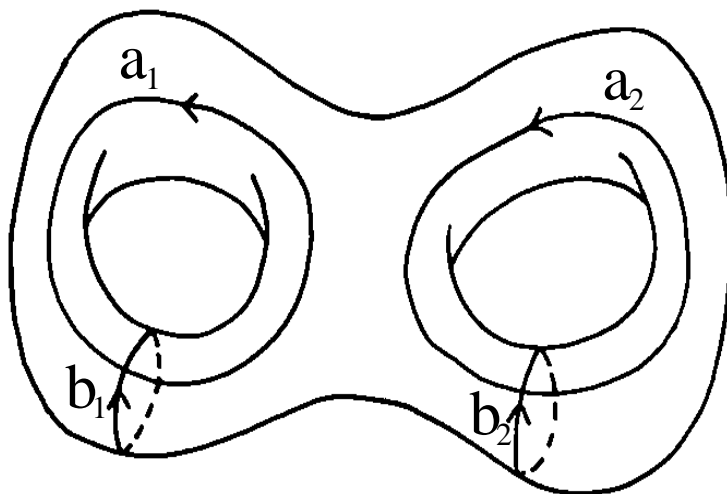
Fig. 7. A genus 2 surface with a canonical basis of cycles.

concept of homology. A cycle is homologous to zero if it bounds a piece of the surface Γ. The sum of two cycles is defined to be the cycle obtained by traversing one cycle after the other following the prescribed orientation (thus a cycle can have multiple components). The negative of a cycle is defined to be the cycle traversed in the opposite direction. Finally, two cycles are homologous to each other if their difference is homologous to zero.

Many of the cycles around holes and handles are deformable into each other, but one easily sees that there are $2g$ cycles which can not be deformed into each other and which are not homologous. Figure. 7 illustrates this for the case of a $g = 2$ surface. As stated in Chapter 1, on a Riemann surface Γ of genus g, it is possible to choose $2g$ nonhomologous cycles such that their intersection indices are as follows:

$$a_i \circ a_j = 0, \quad b_i \circ b_j = 0, \quad a_i \circ b_j = \delta_{ij}, \quad i, j = 0, \ldots, g, \qquad (46)$$

where δ_{ij} is the Kronecker delta: it is one if $i = j$ and zero otherwise. A basis for the homology of the Riemann surface Γ with these intersection indices is called a canonical basis of cycles. Notice that a canonical basis for the homology is not uniquely determined by these intersection conditions.

A combinatorial algorithm for the calculation of a canonical basis for the homology of a Riemann surface specified by its monodromy structure was published by C. L. Tretkoff and M. D. Tretkoff in 1984 [TT84]. The monodromies computed in the previous section allow us to use the methods of [TT84].

Since our implementation follows the Tretkoff & Tretkoff algorithm almost without changes, we limit our discussion of it. Full details may be found in [TT84]. A short geometrical sketch of the algorithm is as follows:

1. Choose a base point $x = a$ as before. In practice, this is the same base point as for the monodromy algorithm.

2. Indicate all places on the Riemann surface Γ, corresponding to $x = a$ contained in $\boldsymbol{y}(a)$. This gives n places $A_i = (a, y_i(a))$, $i = 1, 2, \ldots, n$ on the Riemann surface, which effectively label the sheets of Γ.

3. Let $x = b$ denote a branch point in the complex x-plane. Denote one of the disjoint cycles of σ_b by τ. Then the sheets labeled by A_k, with $k \in \tau$ meet at a branch place B on the Riemann surface, with x-value b. Similarly, each one of the disjoint cycles of any σ_b corresponds one-to-one to a branch place on the Riemann surface, with $x = b$. In particular, the number of branch places on the Riemann surface with $x = b$ is the number of disjoint cycles in σ_b, not including fixed points. The total number of places on the Riemann surface with $x = b$ is the number of disjoint cycles in σ_b, including fixed points. In what follows, we denote the disjoint cycle in σ_b corresponding to B by σ_B.
   Now, on the Riemann surface, indicate all branch places, including branch places at infinity. Let t denote the total number of branch places and B_i, $i = 1, 2, \ldots, t$ the branch places on the Riemann surface.

4. Next join every branch place B_i to each place A_j, for which $j \in \sigma_{B_i}$, $i = 1, \ldots, t$, using paths which only meet at the places B_i and A_j. Thus, every branch place B_i is connected to all places A_j which can be reached by paths emanating from B_i without passing through other branch places B_j, $j \neq i$.
   This creates a non-directed graph on the Riemann surface, with $n + t$ vertices.

5. This graph is reduced to a spanning tree, by removing a number of edges, say r edges. Denote these edges by e_i, $i = 1, \ldots, r$.

6. This spanning tree contains no closed paths, by definition. Adding to it the removed edge e_1 gives rise to a unique closed path on the Riemann surface. Fix an orientation on this closed path, thus defining a cycle c_1.

7. Similarly, every other removed edge e_k gives rise to a closed path on the Riemann surface. If this path has any edges in common with the cycles $c_1, c_2, \ldots, c_{k-1}$, then an orientation is induced from these cycles on the cycle c_k. Otherwise, an orientation is chosen. This way, a collection of r cycles $c_1, \ldots, c_r$ is obtained on the Riemann surface.

Tretkoff and Tretkoff [TT84] show that the cycles constructed above are all nontrivial, i.e., they can not be contracted to a point. Furthermore,

$$r = 2g + n - 1, \tag{47}$$

where g is the genus of the Riemann surface.

Since $n > 1$ (otherwise $y(x)$ is a single-valued function), $r > 2g$. Thus the above construction results in more cycles than are required for a basis of the homology, which has dimension $2g$.

In [TT84], Tretkoff & Tretkoff present an algorithmic way to cut the above-mentioned graph on the Riemann surface across the edges $e_1, \ldots, e_r$. This results in a planar graph which contains cut copies of the cycles $c_1, \ldots, c_r$. Tretkoff & Tretkoff [TT84] show how this planar graph is used to find the intersection numbers $K_{ij} = c_i \circ c_j$, $i, j = 1, \ldots, r$, resulting in an $r \times r$ intersection matrix $\boldsymbol{K} = (K_{ij})_{i,j=1}^g = (c_i \circ c_j)_{i,j=1}^g$. Because only $2g$ of the cycles $c_1, \ldots, c_r$ are independent, the rank of this matrix is $2g$. Furthermore, an $r \times r$ matrix $\boldsymbol{\alpha}$ with integer entries and determinant ± 1 exists such that

$$\boldsymbol{\alpha K \alpha}^T = \boldsymbol{J} = \begin{pmatrix} \boldsymbol{0}_g & \boldsymbol{I}_g & \boldsymbol{0}_{g,n-1} \\ -\boldsymbol{I}_g & \boldsymbol{0}_g & \boldsymbol{0}_{g,n-1} \\ \boldsymbol{0}_{n-1,g} & \boldsymbol{0}_{n-1,g} & \boldsymbol{0}_{n-1,n-1} \end{pmatrix}, \tag{48}$$

with $\boldsymbol{0}_g$ being the $g \times g$ zero matrix, $\boldsymbol{I}_g$ the $g \times g$ identity matrix and $\boldsymbol{0}_{p,q}$ the $p \times q$ zero matrix. We now define the cycles

$$a_i = \sum_{j=1}^r \alpha_{ij} c_j, \quad b_i = \sum_{j=1}^r \alpha_{i+g,j} c_j, \quad i = 1, \ldots, g. \tag{49}$$

It is straightforward to check that these cycles satisfy (46). Hence the cycles $a_1, \ldots, a_g$, $b_1, \ldots, b_g$ define a canonical basis of cycles for the homology of the Riemann surface. The non-uniqueness of such a basis is a restatement of the non-uniqueness of the matrix $\boldsymbol{\alpha}$. This matrix is the transformation matrix from the basis of cycles $c_1, \ldots, c_r$ to the canonical basis. Its first $2g$ rows prescribe the linear combination of the cycles $c_1, \ldots, c_r$ which results in the canonical basis. Its last $n - 1$ rows confirm the dependence of the cycles $c_1, \ldots, c_r$:

$$\sum_{j=1}^r \alpha_{ij} c_j = 0, \quad i = 2g + 1, \ldots, 2g + n - 1. \tag{50}$$

Example. In the following example, we compute a canonical basis for the homology of the Riemann surface of genus 3 corresponding to $y^3 - (x^2 + y)^2 + 1 = 0$. Note that the example is a little different from that used to illustrate the use of the monodromy command, so as to demonstrate what happens when $x = \infty$ is a branch point. The command `homology(f,x,y)` results in a table. This table has the following entries:

1. `basepoint:` the base point $x = a$ for the analytic continuation of the algebraic covering $y(x)$.
2. `sheets:` the ordered n-tuple $\boldsymbol{y}(a)$.

3. `cycles:` the cycles $c_1, c_2, \ldots, c_r$. The cycles are given as lists. The first element of the cycle c_k specifies the starting sheet $y_i(a)$, by displaying i. The second element is a branch point $x = b$ in the complex x-plane, together with the disjoint cycle of σ_b, which contains i. The third element is a sheet $y_j(a)$, given by j. This part of the cycle c_k is read as: "From sheet i proceed to sheet j, by encircling the point $x = b$". It is possible that $x = b$ needs to be encircled more than once, in order to get from sheet i to sheet j. Having arrived at sheet j, this process now repeats. The list is cyclical, meaning that after encircling the last branch point, one arrives again at the initial sheet, so as to obtain a cycle on the Riemann surface.
4. `linearcombination:` the first $2g$ rows of the matrix $\boldsymbol{\alpha}$, as discussed above.
5. `canonicalcycles:` the result of combining `linearcombination` and `cycles`. Each of the cycles $a_1, \ldots, a_g$, $b_1, \ldots, b_g$ is given as a list of lists. Adding the lists in the list gives a basis element of the canonical basis of cycles. Usually, only one list is necessary for each canonical-basis element. Since the canonical-basis elements are obtained from the information in both `cycles` and `linearcombination`, their representation is typically more complicated. Also, instead of specifying the disjoint cycle of the permutation at the branch point, the number of times one needs to encircle the branch point in the complex x-plane counterclockwise is given. If this number is negative, the branch point needs to be encircled clockwise as many times as the absolute value of the number.
6. `genus:` this entry gives the genus of the Riemann surface, by halving the dimension of the canonical basis. This topological calculation is completely independent of the one using Puiseux expansions, used by the `genus` algorithm [vH95] discussed in Section 6.

```
># load the algcurves package
>with(algcurves):
># define the algebraic curve
>f:=y^3-(x^2+y)^2+1=0:
># calculate the homology of the Riemann surface
># corresponding to f.
>h:=homology(f,x,y):
># the base point x=a
>h[basepoint];
```

$$-1.46431608476$$

```
># the sheet labels y(a)
>h[sheets];
```

$$[-.951818492315 - .577121407841i, -.951818492315 + .577121407841i,$$
$$2.90363698463]$$

```
>#  the cycles c_1,...,c_r
>eval(h[cycles]);
```

$\text{table}([1 = [1, [-.256859579359 - 1.04991843161i, [1, 2]],$
$\qquad 2, [-1.22951879712, [1, 2]]],$
$\quad 2 = [1, [1.22951879712, [1, 3]], 3, [.256859579359 + 1.04991843161i, [1, 3]]],$
$\quad 3 = [1, [-.256859579359 - 1.04991843161i, [1, 2]],$
$\qquad 2, [-.256859579359 + 1.04991843161i, [1, 2]]],$
$\quad 5 = [1, [1.22951879712, [1, 3]], 3, [\infty, [1, 2, 3]]],$
$\quad 4 = [1, [-.256859579359 - 1.04991843161i, [1, 2]], 2, [\infty, [1, 2, 3]]],$
$\quad 7 = [1, [-.256859579359 - 1.04991843161i, [1, 2]],$
$\qquad 2, [-.642525578033, [2, 3]], 3, [1.22951879712, [1, 3]]],$
$\quad 6 = [1, [-.256859579359 - 1.04991843161i, [1, 2]],$
$\qquad 2, [.256859579359 - 1.04991843161i, [2, 3]], 3, [1.22951879712, [1, 3]]],$
$\quad 8 = [1, [-.256859579359 - 1.04991843161i, [1, 2]],$
$\qquad 2, [.642525578033, [2, 3]], 3, [1.22951879712, [1, 3]]])$

```
>#  the first 2g rows of the matrix alpha:
>h[linearcombination];
```

$$\begin{pmatrix} 1 & 0 & 0 & 0 & 0 & 0 & 0 & 0 \\ 0 & 1 & 0 & 0 & 0 & 0 & 0 & 0 \\ 0 & 0 & 1 & -1 & 0 & 0 & 0 & 0 \\ 0 & 0 & 0 & 0 & 1 & 0 & 1 & 0 \\ 1 & 0 & 0 & 0 & 1 & 0 & 0 & 0 \\ 0 & 0 & 0 & 1 & -1 & 0 & -1 & 0 \end{pmatrix}$$

```
>#  the canonical-basis cycles
>eval(h[canonicalcycles]);
```

$\text{table}([b[1] = [[1, [-.256859579359 - 1.04991843161i, 1],$
$\qquad 2, [-.642525578033, 1], 3, [\infty, 1]]],$
$\quad a[3] = [[1, [\infty, 1], 2, [-.256859579359 + 1.04991843161i, -1]]],$
$\quad a[2] = [[1, [1.22951879712, 1], 3, [.256859579359 + 1.04991843161i, -1]]],$
$\quad a[1] = [[1, [-.256859579359 - 1.04991843161i, 1], 2, [-1.22951879712, -1]]],$
$\quad b[2] = [[1, [-.256859579359 - 1.04991843161i, 1],$
$\qquad 2, [-1.22951879712, -1], 1, [1.22951879712, 1], 3, [\infty, 1]]],$
$\quad b[3] = [[2, [\infty, 1], 3, [-.642525578033, -1]]]$
$\qquad])$

Thus, the cycle c_1 is as follows: start on sheet 1 (thus $x = -1.46431608476$, $y = -0.951818492315 - 0.577121407841\mathrm{i}$); encircle branch point $x = -0.256859579359 - 1.04991843161\mathrm{i}$ to arrive at sheet 2 (thus $x = -1.46431608476$, $y = -0.951818492315 + 0.577121407841\mathrm{i}$); encircle branch point $x = -1.22951879712$ to arrive back at sheet 1 (thus $x = -1.46431608476$, $y = -0.951818492315 - 0.577121407841\mathrm{i}$, once again).

Using the linear combination matrix from the above example, the cycle b_1 is given by $b_1 = c_5 + c_7$, which is rewritten as: start from sheet 1 ($x = -1.46431608476$, $y = -0.951818492315 - 0.577121407841\mathrm{i}$); encircle branch point $x = -0.256859579359 - 1.04991843161\mathrm{i}$ once counterclockwise, ending up at sheet 2 ($x = -1.46431608476$, $y = -0.951818492315 + 0.577121407841\mathrm{i}$); encircle branch point $x = -0.642525578033$ one time counterclockwise, and end up at sheet 3 ($x = -1.46431608476$, $y = 2.90363698463$); encircle branch point $x = \infty$ one time counterclockwise, and find yourself back at sheet 1 (back at $x = -1.46431608476$, $y = -0.951818492315 - 0.577121407841\mathrm{i}$). Remember that any negative "encircling numbers" imply that the branch point should be encircled clockwise, as is necessary, for instance, for cycle a_3.

Remarks

- Our implementation of the Tretkoff & Tretkoff algorithm [TT84] in "algcurves" is not the first program to implement this algorithm [TT84]. Such a program in Turbo Pascal was already announced in [BT92]. A rewrite in C++ was also communicated to the authors in 1999 [BT99]. These programs start from a representation of the monodromy group of a Riemann surface and construct from it a canonical basis for the homology. To the best of our knowledge, the Maple program `homology`, presented here, is the only program that calculates a canonical basis for the homology of an arbitrary compact connected Riemann surface, starting from the equation of a plane algebraic curve.
- Since it is entirely combinatorial, the homology algorithm is guaranteed to return the correct result if it received the correct input in the form of the monodromy structure of a plane algebraic curve. The algorithm relies on the monodromy algorithm, which may require the user to increase the default accuracy, as discussed in the Remarks at the end of Sect. 7.

9 Holomorphic 1-forms on a Riemann Surface

A basis for the holomorphic 1-forms on a Riemann surface specified by an algebraic curve is given by the span of $\{\omega_1, \ldots, \omega_g\}$, where $\omega_1, \ldots, \omega_g$ are linearly independent holomorphic differentials on the surface. Consider the case of the extended complex x-plane, *i.e.*, the Riemann sphere. Let $R(x)$ be a non-zero meromorphic function on the Riemann sphere. Since meromorphic functions on the Riemann sphere are rational functions, $R(x) = p_n(x)/q_m(x)$, with $p_n(x)$ and $q_m(x)$ polynomials in x of degrees n and m respectively. Then

$\omega = R(x) \, \mathrm{d}x$ is by definition a meromorphic differential on the Riemann sphere, *i.e.*, a differential whose only singularities are poles. This differential has poles at the roots of $q_m(x)$. Hence, in order for ω to be holomorphic, $q_m(x)$ is constant. Without loss of generality, let $q_m(x) = 1$. Furthermore, using $\tau = 1/x$ as a local parameter at $x = \infty$, we can write $\omega = -p_n(1/\tau) \, \mathrm{d}\tau / \tau^2$ at infinity. Hence ω has a pole at infinity unless $p_n(1/\tau)$ has at least a double root at $\tau = 0$, but this is impossible. Thus on the Riemann sphere no non-zero holomorphic differentials exist. However, for genus greater than zero, the situation is different; non-zero holomorphic differentials do exist.

The holomorphic differentials are all of the form (see [BK86] or [Noe83])

$$\omega_k = \frac{P_k(x,y)}{\partial_y f(x,y)} \mathrm{d}x. \tag{51}$$

Here $P_k(x,y) = \sum_{i+j \le d-3} c_{kij} x^i y^j$ is a polynomial in x and y of degree at most $d - 3$, where as before d is the degree of $f(x,y)$ as a polynomial in x and y. Clearly there are no more than $(d-1)(d-2)/2$ linearly independent polynomials $P_k(x,y)$ of this form. These polynomials are referred to as the *adjoint polynomials*. If the curve $\hat{\Gamma}$ (recall, $\hat{\Gamma}$ is the compactified algebraic curve, whose corresponding Riemann surface is Γ) is nonsingular, then all polynomials $P(x,y)$ of degree $\le d - 3$ give rise to a holomorphic differential $\omega = P(x,y)/\partial_y F(x,y) \, \mathrm{d}x$. This is of course consistent with the genus of a nonsingular plane algebraic curve of degree d being exactly $(d-1)(d-2)/2$ [BK86], as was already stated in Section 6.

The denominator $\partial_y F(x,y)$ vanishes at the branch points of $y(x)$ as well as at the singular points, whereas the differential $\mathrm{d}x$ vanishes (using local coordinates) only at the branch points of $y(x)$. Therefore, in order for the differential ω_k not to have poles at the singular points, the numerator $P_k(x,y)$ has to vanish at the singular points. Noether [Noe83] showed that on the algebraic curve at a singular point P of multiplicity m_P the adjoint polynomial $P_k(x,y)$ vanishes with multiplicity at least $m_P - 1$. Imposing regularity of the differentials (51) at a point P imposes a number of independent linear conditions on the coefficients c_{kij} of the polynomial $P_k(x,y)$. The number of such conditions is equal to the delta invariant δ_P of the singularity P, see Section 5.

For every singular point, there are $m_P(m_P - 1)/2$ linear conditions which are easily computed. These arise from the fact that $P_k(x,y)$ should vanish at P with multiplicity $m_P - 1$. If $\delta_P = m_p(m_P - 1)/2$ this is a sufficient number of linear equations. Otherwise $\delta_P > m_p(m_P - 1)/2$, and more linear equations are required. Singular points P with $\delta_P > m_P(m_P - 1)/2$ are called special singularities. These extra linear conditions are obtained by using the Puiseux expansions at the singular points at sufficiently high order: direct substitution of the Puiseux expansion in the candidate expression for the holomorphic differential results in different combinations of the coefficients that necessarily vanish to avoid the presence of singular behavior. Singular points at infinity

require a similar treatment, after representing the plane algebraic curve in homogeneous coordinates and equating one of those coordinates (not Z) to 1.

A different way to obtain the adjoint polynomials is through the use of the Newton polygon [Nov01]. Given the equation $f(x, y) = 0$ for the algebraic curve $\hat{\Gamma}$, its Newton polygon $\mathcal{N}(\hat{\Gamma})$ is the convex hull of all points in the (i, j) plane for which the coefficient of $x^i y^j$ in the equation is nonzero. For each interior point (i, j) (not including boundary points) of $\mathcal{N}(\hat{\Gamma})$, one may construct a meromorphic differential

$$\omega_{ij} = \frac{x^{i-1} y^{j-1}}{\partial_y f(x, y)} \mathrm{d}x. \tag{52}$$

If the algebraic curve is nonsingular, the number of differentials so obtained is exactly g, and all are holomorphic [Nov01]. However, if the curve is singular, linear combinations of these differentials have to be identified that are holomorphic in each set of local coordinates. As above, using the Puiseux expansions at the singular points, this leads to a sufficient number of linear conditions on the coefficients of these linear combinations. As the following example shows, this approach has the advantage that generically fewer candidate differentials are found, simplifying the calculations to incorporate the behavior at the singularities.

Example. We use the familiar example of a hyperelliptic curve to illustrate the above two approaches. Let

$$f(x, y) = y^2 - P_{2g+1}(x), \tag{53}$$

where $P_{2g+1}(x)$ is a polynomial of degree $2g + 1$ in x, with only single roots. The corresponding algebraic curve has genus g [Gri89], and there is only one singular point, namely at infinity.

Using the first approach, our candidate holomorphic differentials are

$$\omega_k = \frac{P_k(x, y)}{y} \mathrm{d}x, \tag{54}$$

where $k = 1, \ldots, (d-1)(d-2)/2$, with $d = 2g + 1$. Thus there are $(d-1)(d-2)/2 = g(2g-1)$ possible differentials. For large genera, the discrepancy between the number of independent holomorphic differentials and the number of candidate differentials increases quadratically.

On the other hand, using the Newton polygon approach, we obtain

$$\omega_{ij} = \frac{x^{i-1} y^{j-1}}{\partial_y f(x, y)} \mathrm{d}x, \tag{55}$$

where $j = 1$ to avoid the boundary of the polygon, and $i = 1, \ldots, g$. A Newton polygon for the $g = 2$ case is illustrated in Fig. 8. We see that, at least for this simple example, the Newton polygon immediately gives a basis of the holomorphic differentials of the correct dimension.
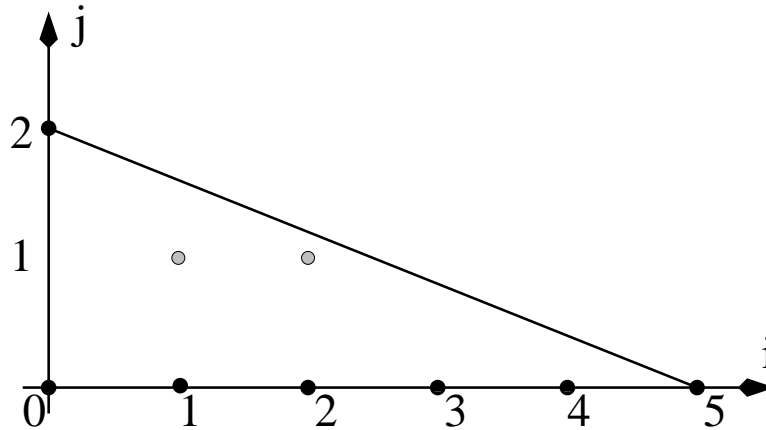
Fig. 8. The Newton polygon for a generic hyperelliptic curve of genus $g = 2$, represented in Weierstrass form.

The `differentials` command from the "algcurves" package uses neither of these approaches. A convenient way to determine the adjoint polynomials $P_k(x, y)$ is described is obtained using a theorem of Mñuk [Mn97]. This way relies on the computation of an integral basis, see Section 4. Denote the set of all adjoint polynomials by $\mathrm{Adj}(\hat{\Gamma})$. The elements of $\mathrm{Adj}(\hat{\Gamma})$ are polynomials $P(x, y) \in \mathbb{C}[x, y]$ for which the differential $\omega = P(x, y)/\partial_y F(x, y) \, \mathrm{d}x$ has no poles in A. Then, for any element $f \in O_{A(\Gamma)}$, $f\omega$ also has no poles in A. In fact one can show that in this case $fP(x, y)$ is again a polynomial, and hence is in $\mathrm{Adj}(\hat{\Gamma})$, see [Mn97]. Denoting by $O_{A(\Gamma)} \cdot \mathrm{Adj}(\hat{\Gamma})$ the set of products of elements of $O_{A(\Gamma)}$ with elements of $\mathrm{Adj}(\hat{\Gamma})$, this statement is written as $O_{A(\Gamma)} \cdot \mathrm{Adj}(\hat{\Gamma}) \subset \mathrm{Adj}(\hat{\Gamma}) \subset \mathbb{C}[x, y]$, since all elements of $\mathrm{Adj}(\hat{\Gamma})$ are by definition polynomials in x and y. Theorem 3.3 of [Mn97] shows that this condition determines the adjoint polynomials completely:

$$\mathrm{Adj}(\hat{\Gamma}) = \{P(x, y) \mid O_A \cdot P(x, y) \subset \mathbb{C}[x, y]\}. \tag{56}$$

Using this result, the linear conditions on the coefficients c_{ij} of $P(x, y) = \sum_{i+j \le d-3} c_{ij} x^i y^j$ arising from the finite singularities are easily found: having found an integral basis $\{\beta_1, \ldots, \beta_n\}$, the above equation is equivalent to demanding that all products $\beta_j P(x, y)$, $j = 1, \ldots, n$ are polynomials in x and y. Using the equation $f(x, y) = 0$, powers of y^n and higher are eliminated from the quantities $\beta_j P(x, y)$. Then these quantities are all reduced to the form $G_j(x, y)/H_j(x)$, with $G_j(x, y)$ a polynomial in x and y, and $H_j(x)$ a polynomial in x. This is rewritten as $G_j(x, y)/H_j(x) = Q_j(x, y) + R_j(x, y)/H_j(x)$, with the degree of $R_j(x, y)$ as a polynomial in x less than the degree of $H_j(x)$. The condition (56) from Mñuk's theorem then states that all coefficients of $R_j(x, y)$ as a polynomial in x and y are zero. These coefficients are linear

combinations of the c_{ij}, and they now are equated to zero. After obtaining similar conditions from the singular points at infinity (see below), the total set of linear equations for the coefficients c_{ij} is solved. The solution set of these equations is g-dimensional, because there are g linearly independent holomorphic differentials and Mñuk proves that (56) completely determines the holomorphic differentials. By computing a set of g independent solutions and substituting these in $P(x,y)$, a set of g linearly independent adjoint polynomials $P_k(x,y)$ is found, and hence by equation (51) a basis $\omega_1, \ldots, \omega_g$ for the holomorphic 1-forms is found.

If $\hat{\Gamma}$ has special singular points at infinity, a similar reasoning applies, but only after transforming (51) such that it is expressed using the coordinate functions $(X/Y, Z/Y)$ or $(Y/X, Z/X)$. Here $(X : Y : Z)$ are the homogeneous coordinates introduced before. Recall that for finite points on $\hat{\Gamma}$, $Z \neq 0$, so that finite points can be denoted by (X, Y), with $Z = 1$. Similarly, for infinite points $Z = 0$, but at least one of X or Y is non-zero. If at a point at infinity $X \neq 0$, then $(X : Y : Z) = (1 : Y/X : Z/X)$. In this case, we equate $X = 1$ and $\hat{y} = Y/X$ and $\hat{z} = Z/X$ are good local coordinate functions near this point at infinity. Otherwise, if $X = 0$ but $Y \neq 0$, then $\tilde{x} = X/Y$ and $\tilde{z} = Z/Y$ are good local coordinates. In the first case, the differential is transformed to the new coordinate functions using $x = X/Z = 1/\hat{z}, y = Y/Z = \hat{y}/\hat{z}$. In the second case, the transformation is $x = X/Z = \tilde{x}/\tilde{z}$, $y = Y/Z = 1/\tilde{z}$. This transformation is now applied to the equation for the plane algebraic curve (1) and the equation for the adjoint polynomial $P(x,y) = \sum_{i+j \leq d-3} c_{ij} x^i y^j$. This results in two equations: an equation for the algebraic curve in the new coordinates and a polynomial $\bar{P}$ in the new coordinates, namely the numerator of $P(x,y)$ under the transformation. The coefficients of this new polynomial $\bar{P}$ are linear combinations of the coefficients c_{ij}. Finding an integral basis for the algebraic curve in the new coordinate functions and applying Mñuk's result (56) gives linear conditions on the coefficients c_{ij}, in addition to the ones obtained using the coordinate functions x and y for the finite points.

If for some singular points at infinity $x = 0$, while for others $y = 0$, then this process may have to be repeated a total of three times, using all three sets of coordinate functions (x, y), $(\hat{x}, \hat{z})$ and $(\tilde{y}, \tilde{z})$.

Example. Using $f(x,y) = y^3 + 2x^7 - x^3 y$, we illustrate the above method and construct the holomorphic differentials. From (51), all holomorphic differentials are of the form $\omega = P(x,y)/(3y^2 - x^3)\mathrm{d}x$, with $P(x,y) = \sum_{i+j \leq 4} c_{ij} x^i y^j$ a polynomial in x and y of degree at most 4. This gives rise to 15 undetermined coefficients c_{ij}. Expressed in homogeneous coordinates $(X : Y : Z)$, the singular points are $P_1 = (0 : 0 : 1)$ and $P_2 = (0 : 1 : 0)$. The second singular point P_2 is infinite and the conditions it imposes on the coefficients of $P(x,y)$ are derived after we find the conditions imposed from P_1.

The multiplicity of $P_1 = (0 : 0 : 1)$ is $m_{P_1} = 3$, its delta invariant is $\delta_{P_1} = 4$. Since $\delta_{P_1} = 4 > 3 = m_{P_1}(m_{P_1} - 1)/2$, the integral basis method is

used. The integral basis is found (see Section 4) to be $\{1, y/x, y^2/x^3\}$. Hence all elements of O_A are of the form $f = f_1(x) + f_2(x)y/x + f_3(x)y^2/x^3$, where $f_j(x)$, $j = 1, 2, 3$ are polynomials in x.

The integral basis gives rise to the conditions that $P(x, y)$, $yP(x, y)/x$ and $y^2P(x, y)/x^3$ are polynomials in x and y. Clearly only the last two of these result in any conditions on the coefficients. Demanding that $yP(x, y)/x$ is a polynomial in x and y, gives $c_{00} = 0 = c_{01}$. Demanding that $y^2P(x, y)/x^3$ is a polynomial in x and y gives $c_{10} = 0 = c_{20}$. As expected, the singular point P_1 results in $\delta_{P_1} = 4$ conditions on the coefficients c_{ij}.

We now turn to the singular point at infinity $P_2 = (0 : 1 : 0)$. Since $y_{P_2} \neq 0$, $(\tilde{x}, \tilde{z})$ are good coordinate functions near this point. After homogenizing $y^3 - x^7 + 2x^3y = 0$ and equating $Y = 1$, we find $\tilde{z}^4 + 2\tilde{x}^7 - \tilde{x}^3\tilde{z}^3 = 0$ and this algebraic curve now has a singular point at $(\tilde{x}, \tilde{z}) = (0, 0)$. The transformed adjoint polynomial is $\bar{P}(\tilde{x}, \tilde{z}) = \sum_{i+j \leq 4} c_{ij}\tilde{x}^i\tilde{z}^{4-(i+j)}$. Again, the integral basis method is used, since $\delta_{P_2} = 9 > 6 = m_{P_2}(m_{P_2}-1)/2$. An integral basis is $\{1, \tilde{z}/\tilde{x}, \tilde{z}^2/\tilde{x}^3, \tilde{z}^3/\tilde{x}^5\}$. Imposing that $\tilde{z}\bar{P}(\tilde{x}, \tilde{z})/\tilde{x}$, $\tilde{z}^2\bar{P}(\tilde{x}, \tilde{z})/\tilde{x}^3$ and $\tilde{z}^3\bar{P}(\tilde{x}, \tilde{z})/\tilde{x}^5$ are polynomials in $\tilde{x}$ and $\tilde{z}$ demands that all $c_{ij} = 0$, except c_{30} and c_{11}, which are undetermined. Hence the most general adjoint polynomial is

$$P(x, y) = c_{11}xy + c_{30}x^3. \tag{57}$$

Thus a basis of holomorphic differentials for the Riemann surface specified by $y^3 + 2x^7 - x^3y = 0$ is

$$\omega_1 = \frac{xy}{3y^2 + 2x^3}\mathrm{d}x, \quad \omega_2 = \frac{x^3}{3y^2 + 2x^3}\mathrm{d}x, \tag{58}$$

which provides an independent confirmation that the genus of the Riemann surface considered in this example is $g = 2$. The calculation of the holomorphic differentials of the Riemann surface specified by $y^3 + 2x^7 - x^3y = 0$ using Maple is given below.

```
># load the algcurves package
>with(algcurves):
># define the algebraic curve
>f:=y^3+2*x^7-x^3*y:
># calculate the holomorphic differentials
>differentials(f,x,y);
```

$$\left[\frac{x^3 dx}{3y^2 - x^3}, \frac{xy dx}{3y^2 - x^3}\right]$$

10 Period Matrix of a Riemann Surface

The values of the integrals of the holomorphic 1-forms along the cycles of the homology are closely related to the geometric and analytic structure of the Riemann surface under consideration [Sie88]. In fact, Torelli's theorem [Gri89] states that, up to isomorphisms, a Riemann surface is determined by these integrals. The values of the integrals are referred to as the periods of the holomorphic differentials. Given bases of both the homology $\{a_i, b_i, i = 1, \ldots, g\}$ and for the holomorphic 1-forms $\{\omega_i, i = 1, \ldots, g\}$, a period matrix $\boldsymbol{\Omega}$ of the Riemann surface Γ is given by

$$\boldsymbol{\Omega} = (\boldsymbol{A}\ \boldsymbol{B}), \tag{59}$$

which is a $g \times 2g$ matrix, consisting of two $g \times g$ blocks:

$$\boldsymbol{A} = (A_{ij})_{i,j=1}^{g}, \quad A_{ij} = \oint_{a_j} \omega_i, \tag{60}$$

$$\boldsymbol{B} = (B_{ij})_{i,j=1}^{g}, \quad B_{ij} = \oint_{b_j} \omega_i. \tag{61}$$

A canonical basis for the holomorphic 1-forms for a canonical basis of the homology is defined by the normalization

$$\oint_{a_j} \hat{\omega}_i = \delta_{ij}. \tag{62}$$

With this basis of holomorphic 1-forms , $\hat{\boldsymbol{A}} \equiv \boldsymbol{I}$, the $g \times g$ identity matrix. The resulting $\hat{\boldsymbol{B}}$ is called a Riemann matrix. If $(\boldsymbol{A}\ \boldsymbol{B})$ is the period matrix obtained from a non-normalized basis of the holomorphic 1-forms, then a Riemann matrix $\hat{\boldsymbol{B}}$ for the Riemann surface is determined by

$$\hat{\boldsymbol{B}} = \boldsymbol{A}^{-1}\boldsymbol{B}. \tag{63}$$

The Riemann matrix depends on the chosen basis of the homology. This is discussed below. It follows from the Riemann relations [Gri89, Spr57] (a consequence of Stokes' theorem) that the Riemann matrix is symmetric and the eigenvalues of its imaginary part are positive definite. Our algorithm never imposes these conditions on the Riemann matrix, as they do not allow us to make the algorithm more efficient or accurate. As a consequence, the symmetry of the Riemann matrix within the accuracy specified provides an excellent check on the the computational results. The positivity of the eigenvalues of the imaginary part may be checked as well, but requires a little more effort on the part of the user.

Having obtained a canonical basis for the homology and the holomorphic differentials of a Riemann surface using the algorithms of the previous sections, a period matrix is found by evaluation of the integrals (60) and (61). Once a

period matrix is found, a Riemann matrix for the Riemann surface is found from (63).

Using (49),

$$\oint_{a_j} \omega_i = \sum_{k=1}^{r} \alpha_{jk} \oint_{c_k} \omega_i, \quad \oint_{b_j} \omega_i = \sum_{k=1}^{r} \alpha_{g+j,k} \oint_{c_k} \omega_i, \tag{64}$$

and the computation of a period matrix reduces to the computation of the integrals $\oint_{c_k} \omega_i$, $k = 1, \ldots, r$ for the holomorphic differential ω_i. By construction, the cycles c_k consists of line segments and semi-circles in the complex x-plane lifted to the Riemann surface. Each one of these line segments or semi-circles is parameterized by $x = \gamma(t)$, with $0 \le t \le 1$. The lifting of $x = \gamma(t)$, denoted by $y = \tilde{\gamma}(y_0, t)$, is obtained by specifying a starting value y_0 of y (essentially the sheet number), and by analytically continuing this value y_0 along $x = \gamma(t)$. Hence $\tilde{\gamma}(y_0, 0) = y_0$ and $f(\gamma(t), \tilde{\gamma}(y_0, t)) = 0$. Thus we have to numerically evaluate integrals of the type

$$\int_0^1 \frac{P_i(\gamma(t), \tilde{\gamma}(y_0, t))}{\partial_y F(\gamma(t), \tilde{\gamma}(y_0, t))} \gamma'(t) \mathrm{d}t \tag{65}$$

The "algcurves" implementation of our algorithm evaluates these integrals using Maple's numerical integration routine. This has the effect that the user can specify the number of significant digits to be used for the computations. If `Digits` is the number of significant digits the user specified, the command `periodmatrix(f,x,y)` attempts to return the periodmatrix of the Riemann surface specified by the plane algebraic curve $f = F(x, y)$ with at least `Digits`-3 significant digits. If this number of significant digits is not attained, a warning is issued. The numerical evaluation of the integrals is slow, since for every evaluation of the integrand numerical analytic continuation is required. As expected, if the user requires more significant digits more computer time is used.

Example. First we compute a Riemann matrix for the Riemann surface specified by $f(x, y) = y^3 + x^4 + x^2$. The genus of this surface is 2, and thus the surface is hyperelliptic [Gri89]. As the reader may verify, the use of the birational transformation

$$u = \frac{y}{x}, \quad v = \frac{2x^3 + y^3}{x^3} \tag{66}$$

reduces the equation $f(x, y) = 0$ to

$$v^2 = u^6 - 4, \tag{67}$$

which is of the standard form of a hyperelliptic curve of genus 2. Using this, it is possible to calculate the Riemann matrix associated with $f(x, y) = 0$ analytically:

$$\hat{B} = \begin{pmatrix} 1 + \dfrac{2i}{\sqrt{3}} & -1 - \dfrac{i}{\sqrt{3}} \\ -1 - \dfrac{i}{\sqrt{3}} & 1 + \dfrac{2i}{\sqrt{3}} \end{pmatrix}. \tag{68}$$

```
># load the algcurves package
>with(algcurves):
># define the algebraic curve
>f:=y^3+x^4+x^2:
># calculate a period matrix for the Riemann surface
># corresponding to f
>pm:=periodmatrix(f,x,y):
># use only 5 significant digits, for display purposes
>evalf(pm,5);
```

$$\begin{pmatrix} .9999999971 + 1.154700542i & -.9999999950 - .5773502479i \\ -.9999999920 - .5773502773i & 1.000000016 + 1.154700531i \end{pmatrix}$$

```
>PM:=Matrix([[1+2*I/s,-1-I/s],[-1-I/s,1-2*I/s]]);
```

$$\mathrm{PM} := \begin{pmatrix} 1 + \dfrac{2i}{\sqrt{3}} & -1 - \dfrac{i}{\sqrt{3}} \\ -1 - \dfrac{i}{\sqrt{3}} & 1 + \dfrac{2i}{\sqrt{3}} \end{pmatrix}$$

```
> evalf(PM);
```

$$\begin{pmatrix} 1. + 1.154700539i & -1. - .5773502693i \\ -1. - .5773502693i & 1. + 1.154700539i \end{pmatrix}$$

We see that the "algcurves" implementation gives the promised accuracy.

Example. This example computes a period matrix and a Riemann matrix for the Riemann surface specified by the algebraic curve given by $f(x,y) = y^3 + x^4 + x^2 = 0$. Since for this example, an exact answer is not known, the accuracy of the output is estimated by the absolute values of the anti-symmetric part of the Riemann matrix.

```
># load the algcurves package
>with(algcurves):
># define the algebraic curve
>f:=y^3+2*x^7-x^3*y:
># calculate a period matrix for the Riemann surface
># corresponding to f
>pm:=periodmatrix(f,x,y):
># use only 5 significant digits, for display purposes
>evalf(pm,5);
```

$$\begin{pmatrix} -.71618 - .98573i & 1.1588 - 2.3480i & -1.2184i & 1.9715i \\ -1.8496 + .60096i & -1.1431 + 2.7753i & -1.9448i & -1.2019i \end{pmatrix}$$

```
># calculate a Riemann matrix for the Riemann matrix
># corresponding to f
>rm:=evalf(periodmatrix(f,x,y,Riemann),10);
```

$$\begin{pmatrix} .2360680016 + 1.175570489i & -.1180339855 - .3632712593i \\ -.1180339976 - .3632712768i & -.5000000061 + .36327127i \end{pmatrix}$$

```
># load the linalg package
>with(linalg):
># compute the anti-symmetric part of rm
>evalm(rm-transpose(rm));
```

$$\begin{pmatrix} 0 & 0.121 \ 10^{-7} + 0.175 \ 10^{-7} \\ -0.121 \ 10^{-7} - 0.175 \ 10^{-7} & 0 \end{pmatrix}$$

```
># increase the digits used in computations to 20.
>Digits:=20;
># calculate a Riemann matrix using 20 digits.
>rm:=periodmatrix(f,x,y,Riemann):
># compute the anti-symmetric part of rm
>evalm(rm-transpose(rm));
```

$$\begin{pmatrix} 0 & 0.41 \ 10^{-18} + 0.1 \ 10^{-19} \\ -0.41 \ 10^{-18} - 0.1 \ 10^{-19} & 0 \end{pmatrix}$$

If the roles of the coordinate functions x and y are switched, x is regarded as an algebraic function of y, $x = x(y)$. This results in an entirely different monodromy. Thus, the coordinate representation of the homology and which cycles are chosen as basis elements may be completely different. The period matrix computation results in a different but symplectically equivalent period matrix, see Chap. 1.

11 Abel map associated with a Riemann Surface

The Abel map $\boldsymbol{\mathcal{A}}$ from a genus g Riemann surface Γ to its Jacobian $J(\Gamma) = \mathbb{C}^g / \Lambda(\Gamma)$ is defined as

$$\boldsymbol{\mathcal{A}}(P_0, P) = (\mathcal{A}_i(P_0, P))_{i=1}^g, \quad \mathcal{A}_i(P_0, P) = \int_{P_0}^{P} \omega_i, \tag{69}$$

where P_0, P are places on Γ, and ω_i is the i-th normalized holomorphic 1-form. Also, $\Lambda(\Gamma)$ is the fundamental period lattice associated with the Riemann surface:

$$\Lambda(\Gamma) = \{\boldsymbol{M} + \hat{\boldsymbol{B}}\boldsymbol{N}, \ \boldsymbol{M}, \boldsymbol{N} \in \mathbb{Z}^g\}. \tag{70}$$

The same path from P_0 to P is used for all components of $\boldsymbol{\mathcal{A}}(P_0, P)$. In almost all applications, the place P_0 is thought of as fixed, whereas the place P may vary. For the purposes of computing the Abel map, their treatment is the same, since obviously

$$\boldsymbol{\mathcal{A}}(P_0, P) = \boldsymbol{\mathcal{A}}(P_0, Q) + \boldsymbol{\mathcal{A}}(Q, P) = -\boldsymbol{\mathcal{A}}(Q, P_0) + \boldsymbol{\mathcal{A}}(Q, P), \tag{71}$$

where Q is any place on Γ. We choose Q to be the place on the first sheet, above the base point. All Abel map computations are split as in (71), with this fixed choice of Q.

The input of the places P_0 and P is given in terms of Puiseux series. If P_0 and P are regular places, it suffices to specify an (x, y)-pair so that $f(x, y) = 0$. On the other hand, if, for instance, P is not a regular place, it needs to be specified by a Puiseux series of sufficiently high order in order to tell it apart from any other places with the same x-coordinate. Therefore, at least as many terms have to be used as necessary to specify the non-regular place as given by the option 0 in Maple's Puiseux command, see Section 3.

As in the previous section, the integrals of the holomorphic differentials reduce to integrals of the type

$$\int_0^1 \frac{P_i(\gamma(t), \tilde{\gamma}(y_0, t))}{\partial_y F(\gamma(t), \tilde{\gamma}(y_0, t))} \gamma'(t) \mathrm{d}t \tag{72}$$

where this time $\gamma(t)$ is a part of a path from Q to P. This path consists of segments of the cycles c_k, $k = 1, \ldots, r$, for which the integration has already been done (allowing for the use of Maple's `remember` tables, dramatically increases the speed of the implementation of the algorithm), and new segments leading from these cycles to the end point P. As before, $\tilde{\gamma}$ is used to denote the lift of γ to the appropriate sheet. Let us specify these paths in more detail. The paths consist of three main parts:

1. A path C_1, which is followed from Q to $\hat{Q}$, where $\hat{Q}$ lies above the base point on the same sheet as P. The places $P = (x_P, y_P)$ and $Q = (x_Q, y_Q)$ are said to lie on the same sheet if following the standard path (as defined in Section 7) from the point x_Q to x_P leads y_Q to y_P. This first path C_1 connects two regular places, and there is no difficulty involved with using the numerical analytic continuation method, as outlined in Section 7. The only issue remaining is which path C_1 to follow. The path used is the shortest in a graph-theoretic sense: using the result from the monodromy algorithm, a table is made which tabulates which branch points can be used as gateways to go between which sheets. Since the Riemann surface is

connected, it is possible to go from any sheet to any other sheet. The path C_1 is chosen so that the number of branch points to encircle is minimized.

2. A second path C_2 is followed from $\hat{Q}$ to $\hat{P}$, where $\hat{P}$ is the place closest (using the Euclidean distance) to P above any of the paths used on the x-Riemann sphere, see Fig. 9. The beginning and the endpoint of C_2 are regular places, and the numerical analytic continuation is used as before.

3. A third and last path C_3 is followed from $\hat{P}$ to P. This path can always be chosen as a straight-line path, which is what we do. By construction, this path does not pass close to any non-regular place (places above problem points or infinity), unless P is itself close to an irregular point. If P is not close to an irregular place, numerical analytic continuation may be used, as for the above two paths. If P is close to, or is an irregular place, then Puiseux series are used to expand the integrand in a power series of the local parameter t. The integral near the non-regular place is calculated symbolically, using this expansion method. We should remark that it was shown in [Pat07] that the radius of convergence of a Puiseux series around an irregular place is exactly the distance to the next closest irregular place. Once this symbolic method has allowed us to step away from the non-regular point sufficiently far, we again resort to numerical analytic continuation.

Some more remarks are in order about the symbolic integration steps. The integrands under consideration are holomorphic differentials, thus they are regular everywhere. Near a non-regular point, the singular terms are canceled symbolically, leaving us with a regular power series (truncated, of course) to integrate symbolically. The symbolic integration routine may be split in several smaller paths. The method works well in accordance with the above quoted convergence result, even in the case that P is a place at or near infinity. The use of a local parameter transforms any improper integral to a proper one.

The Abel map is only defined modulo the period lattice of Γ. Thus, if the user wishes to check, validate or compare results of the calculation, it is necessary to have an additional command that allows us to reduce vectors modulo the period lattice, so as to obtain a unique representative inside the fundamental cell, *i.e.*, on the Jacobian $J(\Gamma)$. Such a lattice reduction is easily implemented: we wish to write the vector $\boldsymbol{v} \in \mathbb{C}^g$ as

$$\boldsymbol{v} = [\boldsymbol{v}] + [[\boldsymbol{v}]], \tag{73}$$

where $[\,\cdot\,]$ is a lattice vector, and $[[\,\cdot\,]]$ is a vector in the fundamental cell. We have

$$[\boldsymbol{v}] = \boldsymbol{M} + \hat{\boldsymbol{B}}\boldsymbol{N}, \tag{74}$$
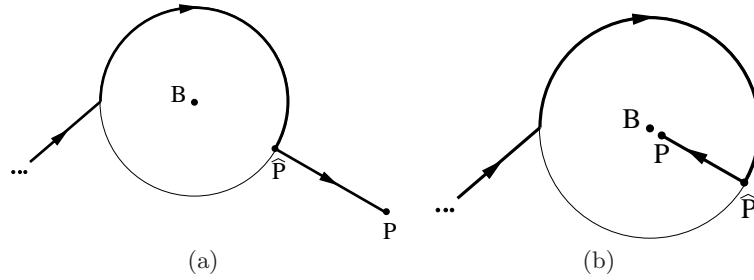
Fig. 9. Paths taken by the Abel transform to the place P. Depicted are lifts of the paths introduced for the monodromy algorithm to the appropriate sheet up to $\hat{P}$. From the $\hat{P}$ to P a straight-line path is used. For (a), the place P is far from any of the non-regular places, and numerical analytical continuation is used. For (b), the place P is too close to the non-regular place B, and a symbolic method using Puiseux expansions is employed.

for some M, $N \in \mathbb{Z}^g$. From the imaginary part of this equation, we easily find N, after which M is found from the real part.

Example. A hyperelliptic curve of genus g may be written in Weierstrass form (see Appendices B and C) as

$$y^2 = P_{2g+1}(x), \tag{75}$$

where $P_{2g+1}(x)$ is a polynomial of degree $2g + 1$. It is known that the Abel map between any two branch points of a hyperelliptic curve is two torsion, *i.e.*, twice the Abel map is a vector in the fundamental lattice $\Lambda(\Gamma)$ [Mum83]. We test this below for the curve

$$y^2 = (x^2 - 1)(x^2 - 4)(x^2 - 9)(x - 4), \tag{76}$$

which has genus 3. The user may wish to refer to Section 3 for the syntax of the command `puiseux`, used below. As the starting place for the Abel map we choose the branch place with $x = -2$. The final place is the branch place at ∞. The command `ModPeriodLattice` is not available in Maple 11, but it, or a command like it, will be available in Maple 12. The user can access code for it from `http://www.amath.washington.edu/~bernard/papers.html`.

```
># load the algcurves package
>with(algcurves):
># define the algebraic curve
>f:=y^2-(x^2-1)(x^2-4)(x^2-9)(x-4):
># define the first place
>P1:=puiseux(f,x=-2,y,0,t)[1];
># define the second place
>P2:=puiseux(f,x=infinity,y,0,t)[1];
```

```
># we compute the Abel map from P1 to P2 with 10 digits of
># accuracy
>V:=AbelMap(f,x,y,P1,P2,t,10);
```

$$[.4782132267 - .6857777356i, .04205771245 + .2852729945i,$$
$$.03629471563 - .2163228835i]$$

```
># We compute the Riemann matrix B, to define the lattice.
>B:=periodmatrix(f,x,y,'Riemann'):
># Now we reduce. With the option 'fraction' the command ModPeriodLattice
># returns the coefficients of the linear combination of
># lattice vectors that is equal to the lattice reduced
># vector.
>W:=ModPeriodLattice(2*V,B,'fraction');
```

$$\big[.99999922115566032, .879 \ 10^{-7}, .99999996924885282, .824 \ 10^{-7},$$
$$.490957264234290476 \ 10^{-7}, .895170631038744930 \ 10^{-7}\big]$$

Up to small errors, these coefficients are all integers, implying that $2V$ is indeed a lattice vector.

Example. As a second example, we compute the Abel map of the divisor of a meromorphic function on a Riemann surface. By Abel's theorem, the resulting Abel map should be a point in the fundamental cell.

Consider the Riemann surface defined by

$$f(x, y) = y^8 + xy^5 + x^4 - x^6. \tag{77}$$

This curve is not hyperelliptic, and has genus 8. We choose a meromorphic function y which has 6 zeros and 6 poles. We leave the calculation of its divisor to the reader. The divisor is

$$D(y) = \left(-1 + \frac{t^5}{2}, t\right) + \left(1 + \frac{t^5}{2}, t\right) + (-t^3, t) + 3\left(t^5, -t^3\right)$$
$$-3\left(-\frac{1}{t^4}, -\frac{1}{t^3} + \frac{t^2}{8}\right) - 3\left(\frac{1}{t^4}, \frac{1}{t^3} + \frac{t^2}{8}\right). \tag{78}$$

We have used truncated Puiseux series to denote the different places in the divisor. Thus, t is a local parameter, defined near $t = 0$, where the actual place is. Below we define these points, and compute the Abel map of this divisor. Next, we reduce the resulting vector modulo the period lattice, to confirm Abel's theorem for this example.

```
># load the algcurves package
>with(algcurves):
># define the algebraic curve
>f:=y^8+x*y^5+x^4-x^6:
>genus(f,x,y);
```

$$8$$

```
># define the first place
>P[1]:=[x=-1+t^5/2,y=t]:
># define the second place
>P[2]:=[x=1+t^5/2,y=t]:
># define the third place
>P[3]:=[x=-t^3,y=t]:
># define the fourth place
>P[4]:=[x=t^5,y=-t^3]:
># define the fifth place
>P[5]:=[x=-1/t^4,y=-1/t^3+t^2/8]:
># define the sixth place
>P[6]:=[x=1/t^4,y=1/t^3-t^2/8]:
># define the multiplicities of all the places
>mult:=[1,1,1,3,-3,-3]:
># a starting point
>P0:=op(allvalues(puiseux(f,x=3,y,0,t))[1]);
```

$$\text{P0} := [x = t + 3, y = \text{RootOf}(\_Z\char`\^8 + 3\_Z\char`\^5\text{-}648, \text{index} = 1)]$$

```
># Now we compute the Abel map of this divisor
>V:=add(mult[k]*AbelMap(f,x,y,P0,P[k],t,10));
```

$$
\begin{aligned}
V := [\ & -1.299153227 - 0.6624504705i, -0.2781898109 - 0.2041198002i, \\
& 1.043210043 - 1.236099255i, 0.2796159734 + 0.4278560587i, \\
& 0.2308962889 + 1.673495279i, 0.5429291623 - 1.575797812i, \\
& -1.300381962 + 0.6826256767i, 0.1436819475 + 0.0356601776i]
\end{aligned}
$$

```
># We reduce the vector V modulo the period lattice. First
># we compute the Riemann matrix B, to define the lattice.
>B:=periodmatrix(f,x,y,'Riemann'):
># Now we reduce.
>W:=ModPeriodLattice(V,B,'fraction');
```

$$[0.9999998122, 0.9999998812, 0.9999999259,$$
$$0.1429633247 \ 10^{-6}, 0.9999994837, 0.9999999613,$$
$$0.1218 \ 10^{-6}, 0.5789289936 \ 10^{-7}, 0.9999999395,$$
$$0.9999998593, 0.9999999317, 0.9999997945,$$
$$0.9999997974, 0.9999997890, 0.9999995188, 0.9999998646]$$

Up to small errors, these numbers are all integers, implying that V is indeed a lattice vector.

12 Riemann Constant Vector of a Riemann Surface

Often, the Riemann constant vector is first encountered in the context of the Jacobi inversion problem, that is, the problem of finding a set of g places $P_1, \ldots, P_g$ on a Riemann surface Γ of genus g such that $\sum_{i=1}^{g} \mathcal{A}(P_0, P_i) \equiv \boldsymbol{z}$ for a given vector $\boldsymbol{z} \in J(\Gamma)$ and initial place $P_0 \in \Gamma$ [Dub81]. Because of this, the Riemann constant vector appears in all formulas determining finite-gap solutions of integrable equations, see [BBE$^+$94] for examples.

Before continuing, it is convenient to recall the definitions of the Riemann theta function, the m-th symmetric power of a Riemann surface and the divisor of an Abelian differential.

- The Riemann theta function with parametric dependence on a $g \times g$ Riemann matrix $\boldsymbol{B}$ (see Section 10) is given by

$$\theta : \boldsymbol{z} \mapsto \theta(\boldsymbol{z}|\boldsymbol{B}) = \sum_{\boldsymbol{n} \in \mathbb{Z}^g} e^{2\pi i \left(\frac{1}{2}\boldsymbol{n} \cdot \boldsymbol{B}\boldsymbol{n} + \boldsymbol{z} \cdot \boldsymbol{n}\right)}, \tag{79}$$

  where $\boldsymbol{z} \in \mathbb{C}^g$. Next, we let Θ, known as the *theta divisor*, denote the subset on the Jacobian $J(\Gamma)$ such that $\theta(\boldsymbol{z}|\boldsymbol{B}) = 0$. Then the theta divisor is a complex $g - 1$ dimensional sub-manifold of $J(\Gamma)$ [FK92].
- Recall from Chapter 1, that a divisor on a Riemann surface Γ is a set of places with multiplicities. A divisor $\mathcal{D}$ is written as $\mathcal{D} = \sum_j p_j P_j$, where $p_j P_j$ denotes that the place P_j has multiplicity p_j. The degree of a divisor is the sum of its multiplicities, denoted $\deg \mathcal{D} = \sum_j p_j$. A divisor is called effective (or positive) if all its multiplicities are positive. The set of all effective divisors of degree m on Γ is denoted $S^m \Gamma$, this is the m-th symmetric power of Γ.
- The divisor (ν) of an Abelian (or meromorphic) differential ν with zeros at the places $P_1, \ldots, P_m$ with multiplicities $p_1, \ldots, p_m$, and poles at the places $Q_1, \ldots, Q_n$ with multiplicities $q_1, \ldots, q_n$ is given by $(\nu) = \sum_{j=1}^{m} p_j P_j - \sum_{j=1}^{n} q_j Q_j$.

Let $\boldsymbol{z} = (z_1, \ldots, z_g) \in \mathbb{C}^g$, and assume an initial place P_0 is given. Consider the function $\phi : \Gamma \mapsto \mathcal{C}$ given by

$$\phi(P) = \theta(\mathcal{A}(P_0, P) - \boldsymbol{z} - \boldsymbol{K}_{P_0}), \tag{80}$$

where $\boldsymbol{K}_{P_0} = (K_1, \ldots, K_g)$ is defined componentwise by

$$K_i = \frac{1 + \boldsymbol{B}_{ii}}{2} - \sum_{j \neq i} \oint_{a_j} \left(\omega_j(P) \int_{P_0}^{P} \omega_i \right) \tag{81}$$

If ϕ is not identically zero on Γ, then it has g zeros $P_0, \ldots, P_g$ and, up to permutation, these zeroes uniquely solve the Jacobi inversion problem. This is the Riemann Vanishing Theorem [Dub81]. The vector $\boldsymbol{K}_{P_0}$ is called the Riemann constant vector with initial place P_0. The algorithm to compute the Riemann constant vector for an arbitrary place P_0 on a Riemann surface does not use (81), which is too expensive. Instead, it relies on the two ideas described below.

- Given the divisor $\mathcal{D} = (\nu)$ of an Abelian differential ν and any initial place $P_0 \in \Gamma$, the Abel map of the divisor is such that [FK92]

$$-\mathcal{A}(P_0, \mathcal{D}) \equiv 2\boldsymbol{K}_{P_0}, \tag{82}$$

where the Abel map $\mathcal{A}(P_0, \mathcal{D})$ of a divisor $\mathcal{D} = \sum_i p_i P_i$ is defined additively: $\mathcal{A}(P_0, \mathcal{D}) = \sum_i p_i \mathcal{A}(P_0, P_i)$. For convenience, denote by $\mathbb{H}_\Gamma$ the set of half lattice vectors in $J(\Gamma)$. That is,

$$\mathbb{H}_\Gamma = \left\{ \boldsymbol{h} \in J(\Gamma) : \boldsymbol{h} = \left[\!\left[\frac{1}{2}\boldsymbol{M} + \frac{1}{2}\boldsymbol{B}\,\boldsymbol{N} \right]\!\right], \quad \boldsymbol{M}, \boldsymbol{N} \in \mathbb{Z}^g \right\}, \tag{83}$$

where $[\![\boldsymbol{z}]\!]$ is the vector $\boldsymbol{z} \in \mathbb{Z}^g$ reduced modulo the period lattice Λ. We impose an ordering on the set $\mathbb{H}_\Gamma$ such that $\boldsymbol{h}_1$ is the zero vector with $2g$ elements. Otherwise the ordering is arbitrary. Using this notation, the equivalence (82) is rewritten as

$$-\frac{1}{2}\mathcal{A}(P_0, \mathcal{D}) + \boldsymbol{h}_i = \boldsymbol{K}_{P_0}, \tag{84}$$

for an appropriate vector $\boldsymbol{h}_i \in \mathbb{H}_\Gamma$ chosen from the 2^{2g} elements of $\mathbb{H}_\Gamma$. Let us summarize: since we know how to compute Abel maps, the above equation provides us with a finite number of possibilities for the Riemann constant vector. How do we select the correct one? The next paragraph provides a way to characterize the Riemann constant vector.

- Irrespective of the initial place P_0, the Riemann constant vector is the difference between the theta divisor and the image under the Abel map of the $(g-1)$-th symmetric power of Γ [FK92]. That is, $\theta(\boldsymbol{z}) = 0$ if and only if $\boldsymbol{z} \in J(\Gamma)$ may be written as

$$z \equiv \mathcal{A}(P_0, \mathcal{D}) + \boldsymbol{K}_{P_0}, \tag{85}$$

with the divisor $\mathcal{D} \in S^{g-1}\Gamma$. Substituting $\mathcal{D} = (g-1)P_0$ in (85) demonstrates that $\theta(\boldsymbol{K}_{P_0}) = 0$ for all $P_0 \in \Gamma$.

Once the Riemann constant vector of any place P_0 on Γ is known, the Riemann constant vector of any other place P_0' may be computed using the formula

$$K_{P_0'} \equiv K_{P_0} - (g-1)\mathcal{A}(P_0, P_0'). \tag{86}$$

Specifically, to compute $\boldsymbol{K}_{P_0}$ we first compute $\boldsymbol{K}_Q$, where, as before, Q is the place on the first sheet above the base point. Next, we compute the Abel map $\mathcal{A}(P_0, Q)$. Then the desired Riemann constant vector is a simple vector sum. The algorithm to compute the Riemann constant vector $\boldsymbol{\kappa}$ of $Q \in \Gamma$ is outlined below. The general idea is to use the fact that there is exactly one vector $\boldsymbol{h} \in \mathbb{H}_\Gamma$ such that $\theta(\boldsymbol{\kappa} + \boldsymbol{h} + \mathcal{A}(Q, \mathcal{D})) = 0$ for all $\mathcal{D} \in S^{g-1}\Gamma$. We use the following steps:

1. Compute the Riemann matrix associated with Γ as discussed in Section 10.
2. Calculate the divisor (ω) of one of the holomorphic (Abelian of the first kind) differentials ω from Section 9. To do this, consider the holomorphic differential ω and a place Q specified as a Puiseux expansion using the local coordinate t. The place Q is an element of the divisor (ω) with multiplicity q if near Q, the differential ω has the representation $\omega_Q = t^q h(t)dt$, where $h(t)$ is locally holomorphic and $h(0) \neq 0$ [Gri89]. Such places occur only for a finite number of x-values, since a holomorphic differential has exactly $2g - 2$ zeros. Three groups of places are checked for membership in (ω):
   a) The intersection points of $P(x, y) = 0$ with $f(x, y) = 0$, where $\omega = P(x, y)dx/\partial_y f(x, y)$. These are the obvious candidates for the zeros of ω. This is done by calculating the resultant (24) of $P(x, y)$ and $f(x, y)$ to eliminate y and to obtain a polynomial equation in x only. Using Puiseux expansions, places consisting of the roots of this equation and their corresponding y values are substituted in ω to determine their multiplicity.
   b) The places corresponding to the problem points defined in Section 7. Recall that the problem points include branch points, singular points, and the roots of $a_n(x) = 0$. These points may be zeros of ω, due to the presence of the differential dx in ω. As above, substitution of the Puiseux expansions at these places allows us to determine the multiplicity (possibly zero) of zeros of the Abelian differential ω.
   c) Places at infinity. These are treated in a different set of coordinates as usual, following from their description in terms homogeneous coordinates. Their multiplicities are determines as above.

3. Compute the initial candidate for the Riemann constant vector, $\boldsymbol{\kappa}$, given by

$$\boldsymbol{\kappa} = \frac{1}{2}\boldsymbol{\mathcal{A}}(Q, (\omega)) + \boldsymbol{h}_1 = \frac{1}{2}\boldsymbol{\mathcal{A}}(Q, (\omega)). \qquad (87)$$

Using this first candidate, all other candidates are constructed as $\boldsymbol{\kappa} + \boldsymbol{h}_i$ for some $i \in \{2, \ldots, 2^{2g}\}$.

4. Using the methods of [DHB$^+$04], construct $T_\epsilon(\boldsymbol{z})$, an approximation for $\hat{\theta}(\boldsymbol{z}|\boldsymbol{B})$ (the oscillatory part of the Riemann theta function, see [DHB$^+$04]) such that $|T_\epsilon(\boldsymbol{z}) - \hat{\theta}(\boldsymbol{z}|\boldsymbol{B})| \leq \epsilon$.

5. For each of the 2^{2g} possible choices for $\boldsymbol{h}_i$, compute $\tau_i = |T_\epsilon(\boldsymbol{\kappa} + \boldsymbol{h}_i)|$, the approximate absolute value of the oscillatory part of the θ-function evaluated at the candidate Riemann constant vector associated with $\boldsymbol{h}_i$. By (85) and the Uniform Approximation Theorem from [DHB$^+$04], if $\tau > \epsilon$, the candidate is eliminated from the list of potential Riemann constant vectors.

    Note that ϵ in Step 4 is chosen to be fairly large (to minimize the evaluation time of T_ϵ), but sufficiently small to eliminate a relatively large number of candidates. This choice is made heuristically, as obtaining the statistics for arbitrary θ-function values needed for a better choice is more costly than evaluating T_ϵ 2^{2g} times required for this part of the algorithm.

6. If Step 5 did not eliminate all but one candidate Riemann constant vector, further elimination is required. To this end we choose $g - 1$ arbitrary places $P_1, \ldots, P_{g-1} \in \Gamma$. A sequence $\mathcal{D}_1, \mathcal{D}_2, \ldots$ of effective, degree $g - 1$ divisors is formed from these places. If $\boldsymbol{h}_i$ is the correct half-lattice vector, then by (84), $\theta(\boldsymbol{\kappa} + \boldsymbol{h}_i + \boldsymbol{\mathcal{A}}(\boldsymbol{Q}, \boldsymbol{\mathcal{D}_j})) = 0$ for all $\mathcal{D}_j \in \mathcal{D}_1, \mathcal{D}_2, \ldots$. Thus, beginning with $j = 1$ and incrementing j as needed, we compute $\tau_i = |T_\epsilon(\boldsymbol{\kappa} + \boldsymbol{h}_i + \boldsymbol{\mathcal{A}}(Q, \mathcal{D}_j))|$ for all remaining candidates $\boldsymbol{\kappa} + \boldsymbol{h}_i$, eliminating those for which $\tau_i \geq \epsilon$. With each such check, the probability that there remain multiple $\boldsymbol{h} \in \mathbb{H}_\Gamma$ drops, as Θ is a $g - 1$ complex-dimensional submanifold of the g complex-dimensional manifold $J(\Gamma)$. In other words, the algorithm succeeds with probability 1. However, if multiple candidates are retained, the algorithm announces this by returning an error to this effect. Otherwise the algorithm has found exactly one candidate $\boldsymbol{\kappa} + \boldsymbol{h}_i \in \Theta$: this is $\boldsymbol{\kappa} = \boldsymbol{K}_Q$.

The vector $\boldsymbol{K}_Q$ depends only on choices that are made algorithmically, namely the choice of homology basis and the base place A_1 (a place above the base point). Permuting the holomorphic differentials basis induces the same permutation on the indices of $\boldsymbol{K}_Q$, $\boldsymbol{\mathcal{A}}$ and $\boldsymbol{B}$. This is a trivial dependence as it is a mere reordering of the coordinates of $\mathbb{C}^g$, or alternatively, of $J(\Gamma)$.

The "algcurves" package of Maple 11 does not contain an implementation of the algorithm discussed here to compute the Riemann constant vector. However, such an implementation should be included in the release of Maple

12. The following examples work with the `RiemannConstants` command as if it were a regular part of the "algcurves" package already.

Example. We compute the Riemann constant vector of two places on the genus 2 curve defined by $y^3 + 2x^7 - x^3y = 0$.

```
>with(algcurves):
># define the algebraic curve
>f:=y^3+2*x^7-x^3y:
># define the initial place
>P0:=puiseux(f,x=0,y,0,t)[1];
```

$$\left[x = t^2, y = t^3 \right]$$

```
># we compute the Riemann constant vector for P0
># asking for 5 digits of accuracy
>K:=RiemannConstants(f, x, y, P0, 5);
```

$$K := [.954915388\,10^{-1} - .2938926454i, -.5000000019 + .5877852634i]$$

```
># we compute the Riemann matrix B, to define the lattice
>B:=periodmatrix(f,x,y,'Riemann'):
># we compute the oscillatory part of the
># Riemann theta function evaluated at K
>RiemannTheta(K, B, [], .001, output = list)[2];
```

$$.6372315\,10^{-7} - .1058378153\,10^{-7}i$$

```
># RiemannConstants may also be called with the flag 'ZERO'
># which computes the Riemann constant vector of the
># place on sheet one above the base point chosen by the
># monodromy procedure
>K0:=RiemannConstants(f, x, y, 'ZERO', 5);
```

$$K0 := [-.1300434055 - .4090318795i, -.4799342464 + .4016561674i]$$

```
># the oscillatory part of the Riemann theta function
># evaluated at K0
>RiemannTheta(K0, B, [], .001, output = list)[2];
```

$$-.9139985751\,10^{-6} - .1478028554\,10^{-5}i$$
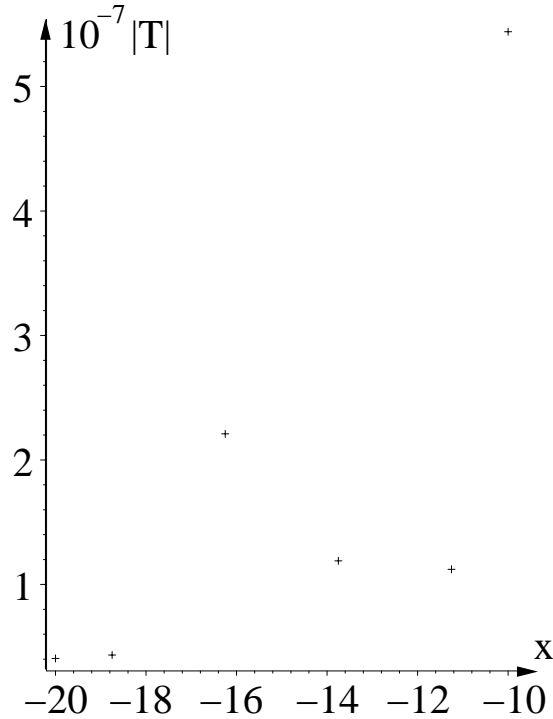
Fig. 10. The absolute value of the oscillatory part of the Riemann theta function evaluated at vectors $K0 + (g − 1)\mathcal{A}(base, P_i)$ as a function of the x coordinate of P_i. The choice of the points P_i is discussed in the main text.

The fact that the absolute values of the oscillatory parts of the Riemann theta function computed in the previous example are small provides no verification that the correct Riemann constant vector has been obtained, since the algorithm chooses the candidates for the Riemann constant vector by enforcing this. We need to verify that the difference, up to numerical error, between the Abel map of the $(g − 1)$-th symmetric power and the theta divisor is indeed equal to our choice for the Riemann constant vector for a set of points on the Riemann surface. This is shown in Figure 10. As both $S^{g−1}\Gamma$ and Θ are strictly lower dimensional submanifolds of $J(\Gamma)$, this demonstrates that the Riemann constant vector was chosen almost surely correct. An approximation of this offset at several arbitrarily chosen points on Γ is computed as follows: we compute a discrete set of points on the genus 2 Riemann surface Γ arising from $y^3 + 2x^7 − x^3y = 0$: we lift the regular points $(−20, −18.75, −16.25, −13.75, −11.25, −10)$, all on the arbitrarily chosen straight line from $−20$ to $−10$ in $\mathbb{C}$, to the places $P_1, \ldots, P_6$ on the first sheet. Next, we compute $V_i = K0 + (g−1)\mathcal{A}(base, P_i)$, where $base$ is the place on Γ chosen during the computation of the monodromy and $K0$ is the Rie-

mann constant vector of *base* computed in the previous example. In Figure 10 we show the points $(x_i, |T(V_i)|)$, where x_i is the x-coordinate of place P_i and T is the approximate absolute value of the oscillatory part of the Riemann theta function. Small numerical error aside, the vectors V_i are in Θ, thus providing numerical confirmation of the correctness of $K0$.

Appendix

Apart from the restriction to an exact representation, all of the algorithms discussed in the previous sections of this chapter are general in the sense that they apply to all compact connected Riemann surfaces. In this appendix, we discuss the use of a few algorithms that apply to restricted classes of algebraic curves and Riemann surfaces, such as elliptic and hyperelliptic surfaces. This appendix contains many examples, but no detailed explanation of the specifics of the algorithms.

1. Parameterizing a Plane Algebraic Curve of Genus Zero

If the genus of an algebraic curve is zero, then this curve can be parameterized in terms of rational functions [Gri89]. A method to construct such a parametrization was given by van Hoeij in [vH97]. This method is implemented as the `parametrization` command in the "algcurves" package. An example of its use is presented below.

Example. Consider the algebraic curve defined by

$$f = y^5 + 2y^4 x - 4x^4. \tag{88}$$

The genus of this curve is zero. We use the `parametrization` command to compute a rational parametrization of the algebraic curve in terms of a parameter t. If the genus of the algebraic curve is not zero, an error is returned.

```
># load the algcurves package
>with(algcurves):
># define the algebraic curve
>f:=y^5+2*y^4*x-4*x^4:
># calculate a rational parametrization for the
># algebraic curve defined by f using a parameter t
>parametrization(f,x,y,t);
```

$$\left[\frac{4}{t^4(2+t)}, \frac{4}{t^3(2+t)} \right]$$

2. When is an Algebraic Curve Hyperelliptic?

An algebraic curve of genus at least 2 is called hyperelliptic if there exists a holomorphic mapping of degree 2 from the curve into the extended complex plane [Gri89]. In practice, hyperelliptic curves stand out from other algebraic curves in the sense that many of their properties resemble those of elliptic curves, including how they may be represented: a hyperelliptic curve is birationally equivalent to a curve of the form

$$v^2 = P_{2g+1}(u), \tag{89}$$

where P_{2g+1} is a polynomial of degree $2g + 1$. This is discussed in the next section. All curves of genus 2 are hyperelliptic [Gri89], but generically, curves of higher genus are not hyperelliptic. A theorem of Max Noether [Noe83] allows one to check when a plane algebraic curve is hyperelliptic, from the knowledge of its holomorphic differentials: let

$$\{f_1(x,y)\mathrm{dx}, \ldots, f_2(x,y)\mathrm{dx}\} \tag{90}$$

denote the set of holomorphic differentials on $\hat{\Gamma}$, defined by $f(x,y) = 0$. Next, one forms the quadratic combinations

$$\{f_i(x,y)f_j(x,y), \ i,j = 1,\ldots,g\}. \tag{91}$$

For a hyperelliptic algebraic curve, exactly $2g-1$ of these functions are linearly independent. For non-hyperelliptic curves, the number of linearly independent functions in this set is greater than $2g - 1$. Noether's theorem was used by van Hoeij to implement the "algcurves" command **is_hyperelliptic**, which determines whether a given plane algebraic curve is hyperelliptic or not.

Example. In this example, we use the is_hyperelliptic command to check whether three plane algebraic curves are hyperelliptic. The first curve has genus 2, thus is hyperelliptic. The next curve has genus 3, and is not hyperelliptic. The last curve has genus three, but is hyperelliptic.

```
>#  load the algcurves package
>with(algcurves):
>#  define the first algebraic curve
>f1:=y^3-2*x*y+x^4:
>#  define the second algebraic curve
>f2:=y^3-2*x*y+x^5:
>#  define the third algebraic curve
>f3:=y^9+3*x^2*y^6+3*x^4*y^3+x^6+y^2:
>#  the genus of the first curve
>genus(f1,x,y);
```

2

```
># thus, the curve is hyperelliptic
>is_hyperelliptic(f1,x,y);
```

<center>true</center>

```
># the genus of the second curve
>genus(f2,x,y);
```

<center>3</center>

```
># this curve is not hyperelliptic
>is_hyperelliptic(f2,x,y);
```

<center>false</center>

```
># the genus of the third curve
>genus(f3,x,y)
```

<center>3</center>

```
># this curve is, in fact, hyperelliptic
>is_hyperelliptic(f3,x,y);
```

<center>true</center>

3. The Weierstrass Form of a Hyperelliptic Algebraic Curve

If an algebraic curve is (hyper)elliptic, it is birationally equivalent to (89), which is known as the Weierstrass form of the hyperelliptic curve. An algorithm to construct the Weierstrass form for an elliptic curve was devised by van Hoeij [vH95], and later extended to hyperelliptic curves. A maple implementation of this algorithm is available in the form of the `Weierstrassform` command in the "algcurves" package. We illustrate its use below.

Example. We use the `Weierstrassform` command to construct the Weierstrass form of the hyperelliptic plane algebraic curve defined by $f_3(x, y)$ in the previous example. The Weierstrass form will be expressed in terms of two new coordinate functions u and v. These are rational functions of x and y. Their inverse $x(u, v)$ and $y(u, v)$ are also rational, and explicitly provided by the algorithm.

```
># load the algcurves package
>with(algcurves):
># define the algebraic curve
>f3:=y^9+3*x^2*y^6+3*x^4*y^3+x^6+y^2:
># the Weierstrass form
>wf:=Weierstrassform(f3,x,y,u,v):
>wf[1];
```

$$v^2 + 2 - 7*u - 35u^3 + 21u^2 + 35u^4 - 21u^5 + 7u^6 - u^7$$

```
>wf[2];                      # u(x,y)
```

$$\frac{y\left(x^2 + y^3 + 1\right)}{y + x^4 + 2x^2y^3 + y^6}$$

```
>wf[3];                      # v(x,y)
```

$$-\frac{x\left(x^2 + y^3\right)}{y}$$

```
>wf[4];                      # x(u,v))
```

$$-(-1 + u)v$$

```
>wf[5];                      # y(u,v)
```

$$1 - 3u + 3u^2 - u^3$$

Acknowledgements

References

[Abh90]   S. S. Abhyankar. *Algebraic geometry for scientists and engineers*, volume 35 of *Mathematical Surveys and Monographs*. American Mathematical Society, Providence, RI, 1990.

[BBE$^+$94]   E. D. Belokolos, A. I. Bobenko, V. Z. Enol'skii, A. R. Its, and V. B. Matveev. *Algebro-geometric approach to nonlinear integrable problems*. Springer Series in Nonlinear Dynamics. Springer-Verlag, Berlin, 1994.

[BK86]   E. Brieskorn and H. Knörrer. *Plane algebraic curves*. Birkhäuser Verlag, Basel, 1986.

[Bli66]   G. A. Bliss. *Algebraic functions*. Dover Publications Inc., New York, NY, 1966.

[BT92]   K. Berry and M. D. Tretkoff. The periodmatrix of macbeath's curve of genus seven. *Contemporary mathematics*, 136:31–40, 1992.

[BT99]   K. Berry and M. D. Tretkoff. Private communication, 1999.

[DFN85]   B. A. Dubrovin, A. T. Fomenko, and S. P. Novikov. *Modern geometry— methods and applications. Part II*, volume 104 of *Graduate Texts in Mathematics*. Springer-Verlag, New York, 1985.

[DHB$^+$04]   B. Deconinck, M. Heil, A. Bobenko, M. van Hoeij, and M. Schmies. Computing Riemann theta functions. 73:1417–1442, 2004.

[DP07a]   B. Deconinck and M. S. Patterson. Computing the Abel map. *Submitted for publication*, 2007.

[DP07b]   B. Deconinck and M. S. Patterson. Computing the Riemann constant vector. *In preparation*, 2007.

[Dub81]   B. A. Dubrovin. Theta functions and nonlinear equations. *Russian Math. Surveys*, 36(2):11–80, 1981.

[DvH01]   B. Deconinck and M. van Hoeij. Computing Riemann matrices of algebraic curves. *Physica D*, 152–153:28–46, 2001.

[FK92]   H. M. Farkas and I. Kra. *Riemann surfaces*. Springer-Verlag, New York, second edition, 1992.

[Gri89]   P. Griffiths. *Introduction to algebraic curves*. American Mathematical Society, Providence, RI, 1989.

[GSST98]   P. Gianni, M. Seppälä, R. Silhol, and B. Trager. Riemann surfaces, plane algebraic curves and their period matrices. *J. Symbolic Comput.*, 26(6):789–803, 1998.

[Mn97]   M. Mñuk. Computing adjoint curves. *J. Symb. Comput.*, 23:229–240, 1997.

[Mum83]   D. Mumford. *Tata lectures on theta. I*, volume 28 of *Progress in Mathematics*. Birkhäuser, Boston, MA, 1983.

[Noe83]   M. Noether. Rationale ausführungen der operationen in der theorie der algebraischen funktionen. *Math. Ann.*, 23:311–358, 1883.

[Nov01]   S. P. Novikov, editor. *Dynamical systems. IV*, volume 4 of *Encyclopaedia of Mathematical Sciences*. Springer-Verlag, Berlin, 2001.

[Pat07]   M. S. Patterson. Algebro-geometric algorithms for integrable systems. *University of Washington Ph.D thesis*, 2007.

[Pot07]   A. Poteaux. Computing monodromy groups defined by plane algebraic curves. *Preprint*, pages 1–13, 2007.

[Rie90]   G. B. Riemann. *Gesammelte mathematische Werke, wissenschaftlicher Nachlass und Nachträge*. Springer-Verlag, Berlin, 1990.

[Sie88]   C. L. Siegel. *Topics in complex function theory. Vol. I.* John Wiley & Sons, Inc., New York, 1988.

[Spr57]   G. Springer. *Introduction to Riemann surfaces.* Addison-Wesley Publishing Company, Inc., Reading, Mass., 1957.

[TT84]   C. L. Tretkoff and M. D. Tretkoff. Combinatorial group theory, Riemann surfaces and differential equations. *Contemporary Mathematics*, 33:467–517, 1984.

[vdW91]   B. L. van der Waerden. *Algebra, Vol. I.* Springer-Verlag, New York, 1991.

[vH94]   M. van Hoeij. An algorithm for computing an integral basis in an algebraic function field. *J. Symb. Comput.*, 18:353–363, 1994.

[vH95]   M. van Hoeij. An algorithm for computing the Weierstrass normal form. In *ISSAC '95 Proceedings*, pages 90–95, 1995.

[vH97]   M. van Hoeij. Rational parametrizations of algebraic curves using a canonical divisor. *Journal of Symbolic Computation*, 23:209–227, 1997.

[vH07]   M. van Hoeij. private communication, 2007.

[Wal62]   R. J. Walker. *Algebraic curves.* Dover Publications Inc., New York, NY, 1962.

Index